ÖGH Herpetozoa
Austrian Herpetological Society

Herpetozoa 38: 271–297 (2025)
DOI 10.3897/herpetozoa.38.e165173

A taxonomic revision of the *Ingerophrynus parvus* species complex (Amphibia, Anura, Bufonidae) with the description of a new species from Thailand

Dmitriy V. Arkhipov[1], Parinya Pawangkhanant[2,3], Goutam Sarker[4,5], Vladislav A. Gorin[1], Andrey M. Bragin[6], Tan Van Nguyen[7,8], Amir Hamidy[9], Mohd Abdul Muin[10], Nia Kurniawan[11], Rafe M. Brown[12], Chatmongkon Suwannapoom[2], Eric Smith[4], Nikolay A. Poyarkov[1]

1 *Department of Vertebrate Zoology, Lomonosov Moscow State University, Leninskiye Gory, Moscow 119234, Russia*
2 *Division of Fishery, School of Agriculture and Natural Resources, University of Phayao, Phayao 56000, Thailand*
3 *Rabbit in the Moon Foundation, Suanphueng, Ratchaburi 70180, Thailand*
4 *Amphibian and Reptile Diversity Research Center (ARDRC) and Department of Biology, The University of Texas at Arlington, Arlington, USA*
5 *Cottey College, 1000 W Austin Blvd, Nevada, MO 64772, USA*
6 *Joint Vietnam - Russia Tropical Science and Technology Research Center, 63 Nguyen Van Huyen Road, Nghia Do, Cau Giay, Hanoi 122000, Vietnam*
7 *The School of Medicine & Pharmacy, Duy Tan University, Da Nang, 550000, Vietnam*
8 *Center for Entomology & Parasitology Research, Duy Tan University, Da Nang, 550000, Vietnam*
9 *Laboratory of Herpetology, Museum Zoologicum Bogoriense, Research Center for Biology, Indonesian Institute of Sciences-LIPI, Widyasatwaloka Jl. Raya Jakarta Bogor km 46, Cibinong, West Java, Indonesia*
10 *Centre for Global Sustainability Studies, Hamzah Sendut Library 1, Universiti Sains Malaysia, 11800 Minden, Penang, Malaysia*
11 *Department of Biology, Universitas Brawijaya, Jl. Veteran, Malang, East Java, Indonesia*
12 *Biodiversity Institute and Department of Ecology and Evolutionary Biology, University of Kansas, Lawrence, KS 66045, USA*

https://zoobank.org/DFF82964-7476-401C-B0FD-D9722A4CCF21

Corresponding authors: Nikolay A. Poyarkov (n.poyarkov@gmail.com); Eric Smith (e.smith@uta.edu); Chatmongkon Suwannapoom (chatmongkonup@gmail.com)

Academic editor: Arthur Tiutenko ♦ **Received** 15 July 2025 ♦ **Accepted** 2 September 2025 ♦ **Published** 1 October 2025

Abstract

A review of the taxonomic status of the *Ingerophrynus parvus* species complex, based on morphological, bioacoustic, and molecular data, revealed a new species from southern Thailand, which we describe as *Ingerophrynus chrysolophus* **sp. nov.** The new species is distinguished from its congeners by the combination of the following morphological characters: parotoid elongate, narrow, and sharply raised; warts on flanks less elevated than those of dorsum; cranial crests not thickened behind eyes; lores vertical; tympanum distinct, its diameter slightly exceeding two-thirds of eye length; tibia short; first finger longer than second; tip of third toe not reaching median subarticular tubercle of fourth toe; subarticular tubercles not enlarged; tarsal spine bases small; nuptial pads present; venter with low warts; ground color of flanks and dorsum light brown; dark brown stripes along the midline of the back; cranial ridges well-developed, bright orange. Phylogenetic analysis of the mtDNA fragment, including the 12S rRNA, 16S rRNA, and ND1 gene sequences (up to 4,479 bp), confirms the placement of the new species as a sister of *Ingerophrynus parvus* **s. str.** (*p*-distance 5.37%). The genetic distinctiveness of *Ingerophrynus chrysolophus* **sp. nov.** and *I. parvus* **s. str.** is further confirmed by not sharing haplotypes of three nuclear genes (POMC, BDNF, and RAG1). Bioacoustic analysis revealed stable differences between the male advertisement calls of the two species. Furthermore, ecological modeling shows that the new species is allopatric with respect to *I. parvus* **s. str.**; their ranges are likely separated by a biogeographical boundary of the Kangar-Pattani Line. The new species is currently known from low- to mid-elevations (ca. 65–1,000 m a.s.l.) in tropical forests of southern and western Thailand, southern Myanmar, and southwest Cambodia. We suggest the new species be considered Least Concern (LC) according to the IUCN Red List criteria. Our study further underscores the urgent need for intensified integrative taxonomic research of the genus *Ingerophrynus* to clarify the taxonomy of wide-ranging species complexes and to elaborate effective conservation measures.

Copyright *Dmitriy V. Arkhipov et al.* This is an open access article distributed under the terms of the Creative Commons Attribution License (CC BY 4.0), which permits unrestricted use, distribution, and reproduction in any medium, provided the original author and source are credited.

Key Words

Asia, integrative taxonomy, Kangar-Pattani Line, morphology, systematics

Introduction

The toad genus *Ingerophrynus* Frost, Grant, Faivovich, Bain, Haas, Haddad, de Sá, Channing, Wilkinson, Donnellan, Raxworthy, Campbell, Blotto, Moler, Drewes, Nussbaum, Lynch, Green & Wheeler, 2006 inhabits tropical forest areas throughout southern mainland China, Hainan Island, and Indochina through Myanmar, peninsular Thailand, the Thai-Malay Peninsula, Sumatra, Borneo, Java, Nias, Sulawesi, and the Philippines (Frost et al. 2006; Frost 2025). The genus *Ingerophrynus* is morphologically diagnosed by the following combination of characters: the presence of supraorbital, parietal, and supratympanic crests; the absence of a tarsal ridge; vocal sacs lacking melanophores in the surrounding muscle tissue; the absence of tibial glands; the absence of supinator manus humeralis and adductor longus muscles; the presence of paired crests on the vertebral column; a rugose skull; squamosal bones with broad dorsal otic plates; and smooth palatine bones (Inger 1972; Grismer 2007). The genus *Ingerophrynus* currently includes 13 recognized species (Frost, 2025), namely, *I. biporcatus* (Gravenhorst, 1829), *I. celebensis* (Günther, 1859), *I. claviger* (Peters, 1863), *I. divergens* (Peters, 1871), *I. galeatus* (Günther, 1864), *I. gollum* Grismer, 2007, *I. kumquat* (Das & Lim, 2011), *I. ledongensis* (Fei, Ye & Huang, 2009), *I. macrotis* (Boulenger, 1887), *I. parvus* (Boulenger, 1887), *I. philippinicus* (Boulenger, 1887), *I. quadriporcatus* (Boulenger, 1887), and *I. wangyingyongi* Liu, Zhang, Ananjeva, Liu, Hou & Orlov, 2025. However, the phylogenetic relationships among the members of the genus *Ingerophrynus* have not been studied extensively, and it is quite likely that its current diversity is underestimated.

The Malayan dwarf toad, *Ingerophrynus parvus* Boulenger, 1887, was described by Boulenger (1887) from the environs of Malacca, Malaysia (Fig. 1). This species has been considered widely distributed across southern Myanmar, southern, western, and eastern Thailand, Cambodia, Peninsular Malaysia, and Indonesia (Poyarkov et al. 2021; Frost 2025). Recent studies have suggested that *I. parvus* may in fact represent a complex of species due to substantial morphological and molecular differences between the populations in the southern and northern parts of the Thai–Malay Peninsula (Mulcahy et al. 2018; Srion et al. 2018; Chan and Grismer 2019).

In this work, we present an updated mitochondrial DNA (hereafter mtDNA) genealogy for the genus *Ingerophrynus*, combining sequences available in GenBank with newly generated sequences obtained from an extensive sampling across Southeast Asia. We further analyze the differentiation within the *I. parvus* species complex using three nuclear DNA (hereafter nuDNA) loci, bioacoustic analysis, and ecological niche modeling. Our results suggest a substantial differentiation of the *I. parvus* species complex populations located on different sides of the Kangar-Pattani Line, an important biogeographical border in Southeast Asia (Poyarkov et al. 2021, 2023). Herein, we provide a taxonomic revision of the *I. parvus* species complex and describe the populations from north of the Kangar-Pattani Line as a new species.

Materials and methods

Sample collection

Fieldwork was carried out in different provinces of Thailand in March and December 2020, January and February 2022, November 2021, February 2024, and July 2024 (Fig. 1). Specimens were collected by hand during excursions along forest trails or near breeding sites, including temporary rain ponds and slow-moving streams. Geographic coordinates and altitude data were accurately captured using a Garmin GPSMAP 60CSx GPS receiver and recorded in the WGS 84 datum. The specimens were euthanized using a 20% benzocaine solution. Prior to preservation, tissue samples were extracted for genetic analysis and stored in 96% ethanol; these samples included either femoral muscles or a piece of liver. Specimens were subsequently fixed in 4% buffered formalin and later transferred to 70% ethanol.

Specimen collection and animal use protocols in Thailand were approved by the Institutional Ethical Committee of the Institutional Ethical Committee of Animal Experimentation of the University of Phayao, Phayao, Thailand (certificate number UP-AE64-02-04-005, issued to C. Suwannapoom) and were strictly compliant with the recommendations of the Thailand Animal Welfare Act. Fieldwork, including the collection of animals in the field, was authorized by the Institute of Animals for Scientific Purpose Development (**IAD**), Bangkok, Thailand (permit numbers U1-01205-2558 and UP-AE59-01-04-0022, issued to C. Suwannapoom). Research in Indonesia was conducted under research permit 149/SIP/FRP/SM/V/2013 (issued to E.N. Smith).

Additional specimens and tissue samples were obtained from museum collections. Specimens and tissues originated from the herpetological collections of the Zoological Museum of Moscow University (**ZMMU**, Moscow, Russia), Rabbit in the Moon Foundation (**RIM**, Suanphueng,

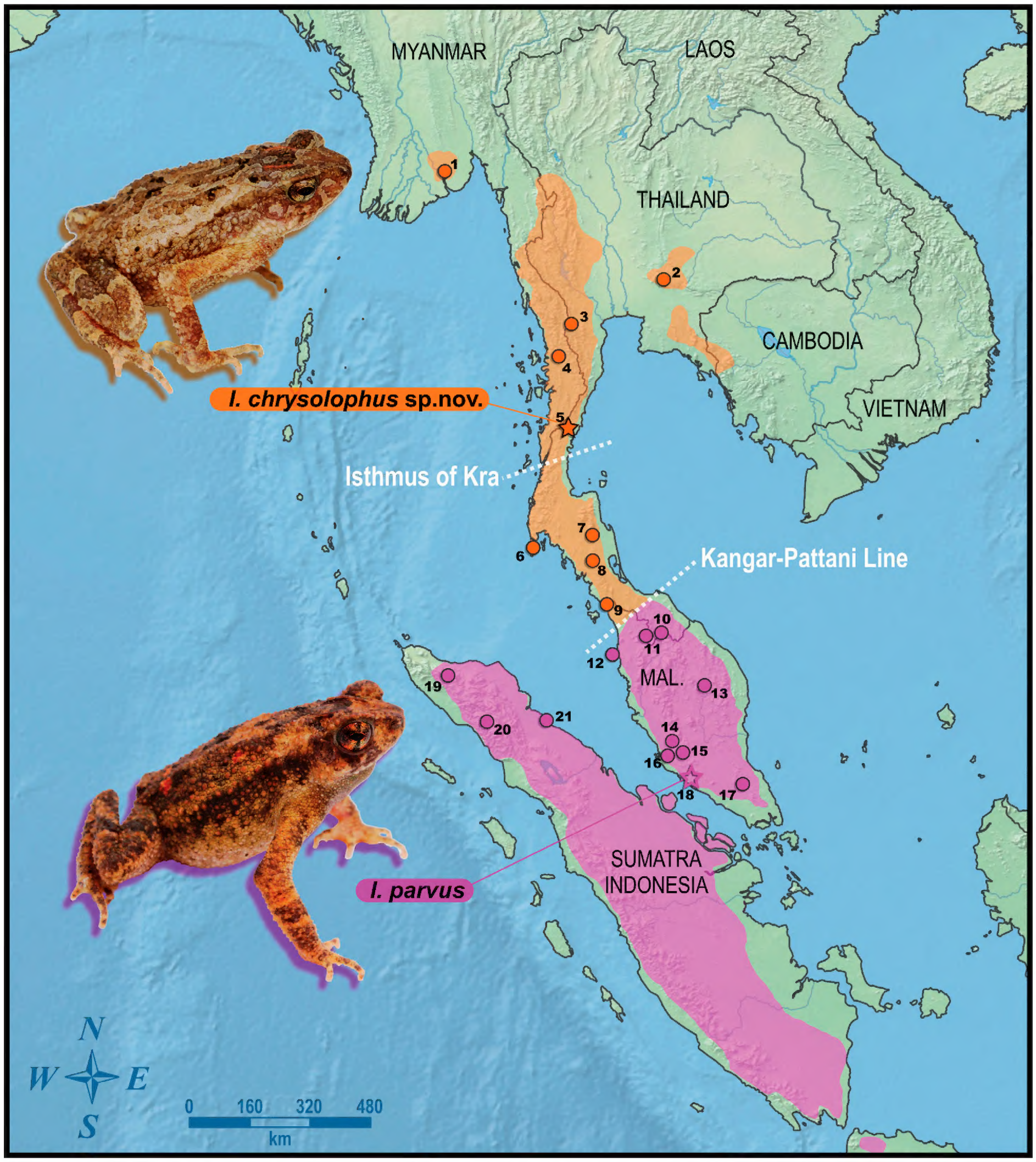

Figure 1. Distribution of the lineages of the *Ingerophrynus parvus* species complex as identified in the phylogenetic analyses. Stars denote type localities, with their corresponding taxon names in colored clouds; colors correspond to those used in Figs 2–5; symbol shapes denote mtDNA lineages shown in Fig. 2. Base map created using simplemappr.net. For locality information, see Suppl. material 1: table S2. Photographs by P. Pawangkhanant and N.A. Poyarkov.

Ratchaburi, Thailand), the School of Agriculture and Natural Resources, the University of Phayao (AUP, Phayao, Thailand), the University of Kansas, Museum of Natural History (KU, Lawrence, Kansas, USA), the University of Texas at Arlington (UTA, Arlington, Texas, USA), and the Kunming Institute of Zoology, Chinese Academy of Sciences (KIZ, Kunming, China). The location of the examined populations and the distribution of the *I. parvus* species complex are shown in Fig. 1.

Laboratory methods

DNA was isolated from the thigh muscles or liver of vouchered specimens. For the molecular phylogenetic analyses, total genomic DNA was isolated using the standard phenol-chloroform-proteinase K extraction procedures with consequent isopropanol precipitation for a final concentration of about 1 mg/ml (protocols followed Hillis et al. 1996; Sambrook and Russell 2001).

We visualized the isolated total genomic DNA using agarose electrophoresis in the presence of ethidium bromide. We measured the concentration of total DNA in 1 µl using NanoDrop 2000 (Thermo Scientific) and consequently adjusted it to ca. 100 ng DNA/µL.

In total, we amplified two fragments of mtDNA and three nuDNA genes. Primers used in PCR and sequencing are summarized in Suppl. material 1: table S1 and were taken from Hedges (1994), Goebel et al. (1999), Wiens et al. (2005), Pramuk (2006), Van der Meijden et al. (2007), Páez-Moscoso and Guayasamin (2012), and Liedtke et al. (2017). We performed DNA amplification in 20 µl reactions using ca. 50 ng genomic DNA, 10 nmol of each primer, 15 nmol of each dNTP, 50 nmol additional $MgCl_2$, Taq PCR buffer (10 mM Tris-HCl, pH 8.3, 50 mM KCl, 1.1 mM $MgCl_2$, and 0.01% gelatin), and 1 unit of Taq DNA polymerase.

First, we amplified a 453 bp long continuous fragment of the 16S rRNA mtDNA gene. This fragment of the 16S rRNA gene is widely used for biodiversity surveys in amphibians (Vences et al. 2005; Vieites et al. 2009) and has been analyzed in the most recent phylogenetic studies of the family Bufonidae (e.g., Smart et al. 2017; Chan and Grismer 2019; Sarker et al. 2019; Suwannapoom et al. 2021, 2022). The PCR conditions involved an initial denaturation step of 5 min at 94 °C, followed by 34 cycles of denaturation for 1 min at 94 °C, primer annealing for 1 min at 50 °C, extension for 1 min at 72 °C, and a final extension step for 5 min at 72 °C.

Additionally, for the selected samples representing different lineages within the genus *Ingerophrynus*, we amplified a 2,100 bp long continuous mtDNA fragment, including partial sequences of the 12S rRNA gene, complete sequences of tRNAVal, 16S rRNA, tRNALeu, and partial sequences of the NADH dehydrogenase subunit 1 gene (ND1). The PCR conditions involved an initial denaturation step of 3 min at 94 °C, followed by 35 cycles of denaturation for 35 s at 94 °C, primer annealing for 40 s at 48 °C, extension for 40 s for 12S rRNA / 60 s for ND1 at 72 °C, and a final extension step for 10 min at 72 °C.

For the selected samples representing different populations within the *I. parvus* species complex, we also amplified three nuDNA genes: POMC, BDNF, and RAG1. Primers used in PCR and sequencing are summarized in Suppl. material 1: table S1. The PCR conditions for the POMC gene were as follows: an initial denaturation step of 3 min at 94 °C, followed by 44 cycles of denaturation for 35 s at 94 °C, primer annealing for 40 s at 54 °C, extension for 40 s at 72 °C, and a final extension step for 10 min at 72 °C. The PCR conditions for the BDNF gene were as follows: an initial denaturation step of 5 min at 94 °C, followed by 32 cycles of denaturation for 1 min at 94 °C, primer annealing for 1 min at 50 °C, extension for 1 min at 72 °C, and a final extension step for 10 min at 72 °C. The PCR conditions for the RAG1 gene were as follows: an initial denaturation step of 5 min at 94 °C, followed by 10 cycles of denaturation for 1 min at 94 °C, primer annealing for 1 min with touchdown temperature from 65 °C to 55 °C, with temperature reducing by 1 °C per each cycle, extension for 1 min at 72 °C, followed by 34 cycles of denaturation for 1 min at 94 °C, primer annealing for 1 min at 55 °C, extension for 1 min at 72 °C, and a final extension step for 10 min at 72 °C.

We ran all amplifications using an iCycler Thermal Cycler (Bio-Rad). We loaded the PCR products onto 1% agarose gels in the presence of ethidium bromide and visualized them by electrophoresis. The successful targeted PCR products were purified by the Diatom DNA PCR Clean-Up kit and outsourced to Evrogen® (Moscow, Russia) for sequencing; sequence data collection and visualization were performed on an ABI 3730xl Automated Sequencer (Applied Biosystems). We deposited the newly obtained sequences in GenBank under the accession numbers PX209002–PX209038 and PX213461–PX213508 (Suppl. material 1: table S2).

Phylogenetic analyses

To reconstruct the matrilineal genealogy of the genus *Ingerophrynus*, we used newly obtained 16S rRNA sequences of *I. parvus* from Thailand and the sequences of the 12S rRNA, 16S rRNA, and ND1 mtDNA fragments of the *I. parvus* species complex members from Thailand, Myanmar, Malaysia, and Indonesia, as well as other *Ingerophrynus* species, obtained from GenBank. Suppl. material 1: table S2 summarizes the information on GenBank accession numbers, museum vouchers, and the locality of origin for the sequences used in this study. We used sequences of ten Asian Bufonidae representatives as outgroups to root the tree, namely *Ansonia leptopus* (Günther, 1872), *Duttaphrynus* cf. *melanostictus* (Schneider, 1799), *Leptophryne borbonica* (Tschudi, 1838), *Phrynoidis juxtasper* (Inger, 1984), *Pelophryne misera* (Mocquard, 1890), *Rentapia hosii* (Boulenger, 1892), *Pseudobufo subasper* Tschudi, 1838, *Sabahphrynus maculatus* (Mocquard, 1890), *Parapelophryne scalpta* (Liu & Hu, 1973), and *Sigalegalephrynus harveyi* Sarker, Wostl, Thammachoti, Sidik, Hamidy, Kurniawan & Smith, 2019, based on the phylogenetic results of Frost et al. (2006), Mulcahy et al. (2018), and Chan and Grismer (2019). In total, we obtained mtDNA data for 65 specimens of *Ingerophrynus*, which included ten out of the 13 currently recognized *Ingerophrynus* species and 44 specimens of the *I. parvus* species complex; the geographic distribution of the sampled populations of the *I. parvus* species complex is shown in Fig. 1.

We initially aligned nucleotide sequences using ClustalX 1.81 (Thompson et al. 1994) with default parameters and then optimized them manually in BioEdit 7.0.5.2 (Hall 1999) and MEGA 11.0 (Tamura et al. 2013). We utilized ModelFinder (Kalyaanamoorthy et al. 2017) to determine the most suitable evolutionary models for our data set analysis; they are presented in Suppl. material 1: table S3. We calculated pairwise uncorrected genetic distances (*p*-distances) between sequences with MEGA 11.0.

We inferred the matrilineal genealogy using Bayesian Inference (**BI**) and Maximum Likelihood (**ML**) approaches. We conducted BI using MrBayes 3.1.2 (Ronquist and Huelsenbeck 2003). Metropolis-coupled Markov chain Monte Carlo (**MCMCMC**) analyses were run with one cold chain and three heated chains for one million generations and sampled every 1,000 generations. We performed two independent MCMCMC runs, and the initial 100 trees were discarded as burn-in. We assessed confidence in tree topology based on the frequency of nodal resolution (posterior probability; BI PP) (Huelsenbeck and Ronquist 2001). We used IQ-TREE (Nguyen et al. 2015) to reconstruct ML trees. A total of 10,000 ultrafast bootstrap replications for ML analysis (**UFBS**) (Minh et al. 2013) assessed the confidence in tree topology for ML analysis. In both datasets, we a priori regarded tree nodes with BI PP values over 0.95 and UF BS values over 95% as strongly supported. We considered BI PP values between 0.95 and 0.90 and UF BS values between 95% and 90% as tendencies, while lower values were considered to indicate the lack of support (Huelsenbeck and Hillis 1993; Minh et al. 2013).

Additionally, for the three nuclear markers examined (POMC, BDNF, and RAG1), we constructed allele networks for each gene using the median-joining method in PopArt ver. 1.5 (Leigh and Bryant 2015) with a 95% connection limit. For the purpose of allele network construction, sequences with more than one heterozygous site were resolved in PHASE 2.1.1 (Stephens et al. 2001), for which the input data were prepared in SeqPHASE (Flot 2010). PHASE was run under default settings, except for the probability threshold, which was set to 0.7.

Morphological examination

Morphometric data were taken for 44 adult males and 32 females of the *Ingerophrynus parvus* species complex (Table 1). Measurements were taken using a Mitutoyo digital caliper to the nearest 0.01 mm and subsequently rounded to 0.1 mm. All measurements were taken on the right side of the examined specimen. The morphometrics of adults and character terminology followed Grismer (2007) and included the following characters: snout-vent length, from tip of snout to vent (**SVL**); head length from tip of snout to hind border of angle of jaw (**HL**); head width, width of head at its widest point (HW); head height in the interorbital region (**HD**); distance from the tip of the muzzle to the nostrils (**S-N**); distance between nostrils (**IND**); distance from nostril to anterior corner of eye (**N-E**); horizontal eye diameter (**ED**); interorbital distance, as the distance between the inner border of the upper eyelid (**IOD**); eyelid width at the widest part (**ELW**); distance between the eye and the tympanic membrane (**ETD**); distance from eyes to tip of snout (**ESD**); horizontal diameter of tympanum (**TD**); cranial crest length (**CRL**); parotoid Width (**PGW**); parotoid gland length (PGL); length of the forelimbs from the base of the forelimb to the tip of the longest finger (**FLL**); length of the forearm and hand from the elbow to the tip of the longest finger (**FHL**); forearm width (**FAW**); hand length from the proximal base of the outer metacarpal tubercle to the tip of the longest finger (**HAL**); 1st finger length (**F1**); 2nd finger length (**F2**); 3rd finger length (**F3**); 4th finger length (**F4**); length of the internal metacarpal tubercle (**IMC**); length of the external metacarpal tubercle (**OMC**); hip length from anus to knee (**FEL**); tibia length, distance between knee and tibiotarsal articulation (**TIL**); tarsus and foot length (**TFL**); foot length from the proximal base of the internal metatarsal from the tubercle to the tip of the longest toe (**FOL**); 1st toe length (**T1**); 2nd toe length (**T2**); 3rd toe length (**T3**); 4th toe length (**T4**); 5th toe length (**T5**); length of the internal metatarsal tubercle (**IMT**); length of the outer metatarsal tubercle (**OMT**). Toe webbing and subarticular tubercle formulas were described following Savage (1975). The sex and maturity of the specimens were checked by minor dissections and examination of gonads and direct observation of calling in living males prior to collection. Other abbreviations: **Dist.** = District; **FR** = Forest Reserve; **Mt** = Mountain; **NP** = National Park; **NR** = Natural Reserve; **Prov.** = Province; **asl.** = above sea level.

Among the examined populations, SVL was compared using a one-way ANOVA with the Tukey-Kramer test. The percentage ratio (R) of each morphometric character to SVL was subsequently calculated; we compared 22 character ratios against SVL among populations using the Kruskal-Wallis test. PCA was conducted to examine overall morphological variation among populations using log-transformed metric values following Nishikawa et al. (2007). When a high correlation between certain pairs of characters was found, we omitted one of them from the analyses to exclude possible overweighting effects. Statistical analyses were performed with Statistica 6.0 (StatSoft Inc. 2001). The significance level was set at $p < 0.05$.

The diagnosis of the genus *Ingerophrynus* and morphological characters for comparison were taken from the original descriptions and taxonomic reviews of the genus: Boulenger (1887), Inger (1966, 1972), Manthey and Grossmann (1997), Das and Lim (2001), Grismer (2007), and Fei et al. (2012).

Species distribution modeling (SDM)

We used the program Maxent 3.4.1 (Phillips et al. 2006; Phillips and Dudik 2008) to model the potential distribution of the *Ingerophrynus parvus* species complex members in Southeast Asia. A total of 155 unique georeferenced data points (Suppl. material 1: table S4) and 19 bioclimatic variables reflecting the height, aspect, and degree of inclination of the Earth's surface; aridity index; vegetation types; the percentage of coverage of the Earth's surface by woody vegetation; and temperature and precipitation data throughout the year (bio1-19) were used to generate the model at 5 km pixel size.

Table 1. Morphometric characters (in mm) recorded from each specimen of *Ingerophrynus parvus* sensu stricto and *Ingerophrynus chrysolophus* sp. nov. examined in this study. Notes: H = holotype, P = paratype, R = referred material, M = adult male, F = adult female. (Continued on the next page).

ZMMU ID	Locality	Status	Sex	SVL	HL	HW	HD	S-N	IND	N-E	ED	IOD	ELW	ETD
Ingerophrynus parvus														
ZMMU A-8029	Yala, Thailand	–	F	48.5	13.8	16.6	6.8	1.7	3.8	3.2	5.3	4.8	4.2	1.1
ZMMU A-8021	Yala, Thailand	–	F	47.9	13.9	15.9	6.6	1.6	3	2.9	6	4.4	4.2	1.1
ZMMU NAP-09684	Selangor, Malaysia	–	F	44.5	13.2	16.9	8.9	1.6	3.2	2.8	5.3	4.9	3.7	0.5
ZMMU A-8025	Yala, Thailand	–	M	33.1	9.8	11.6	5.2	0.9	2.5	2.1	4	3.4	3.1	1.2
ZMMU A-8026	Yala, Thailand	–	M	34.9	9.4	11.2	4.6	1.3	2.3	2.6	4.3	3.6	3.2	0.8
ZMMU A-8024	Yala, Thailand	–	M	33.8	10.2	11.9	4.4	1.3	2.3	2.4	4.4	3.8	3.1	0.9
ZMMU A-8022	Yala, Thailand	–	M	33.5	9.9	11.7	5.3	1.1	2.3	2	4.5	3.1	3.2	0.7
ZMMU A-8023	Yala, Thailand	–	M	36.2	10.1	11.6	4.5	1.2	2.5	2.1	4.9	4	3.1	0.8
ZMMU A-8027	Yala, Thailand	–	M	35.4	9.8	11.8	5.2	1.4	2.5	2.6	4.4	3.9	3	1.1
ZMMU A-8028	Yala, Thailand	–	M	36.7	10.8	12.2	5	1.4	2.5	2.5	4.7	3.9	3.4	0.8
Ingerophrynus chrysolophus **sp. nov.**														
ZMMU A-8035	Chumphon, Thailand	P	F	34.2	10.2	11.8	4.8	1.3	2.4	2.2	4.3	3.3	3.3	0.7
ZMMU A-8030	Chumphon, Thailand	H	F	34.8	10.6	11	3.7	1.9	2.4	2.8	4.7	3.7	3.2	0.7
ZMMU A-8036	Chumphon, Thailand	P	F	35	9.6	10.6	5.2	1.2	2.2	2.5	4.3	3.5	3.2	0.7
ZMMU A-8037	Chumphon, Thailand	P	F	34	9.3	10.6	4.3	1.1	2.2	2.5	4.1	3.7	3.4	0.7
ZMMU NAP-09425	Suan Phueng, Ratchaburi, Thailand	R	F	38.2	10.7	13.4	5.9	1.2	2.3	2.9	4.8	3.6	3.4	1
ZMMU A-8211	Suan Phueng, Ratchaburi, Thailand	R	F	35.3	10.2	12	5.1	1.3	2.4	2.3	4.5	4.1	3.3	0.7
ZMMU A-8061	Suan Phueng, Ratchaburi, Thailand	R	F	36.3	10.5	11.6	5.3	1.5	2.3	2.6	4.2	3.9	3.4	0.8
ZMMU A-8031	Chumphon, Thailand	P	F	39.5	11.2	12.6	5.2	1.5	2.7	2.8	4.1	3.9	3.5	0.8
ZMMU A-8033	Chumphon, Thailand	P	F	37.8	10.4	12.9	5.3	1.6	2.8	2.6	4.8	3.7	3.5	0.9
ZMMU A-8032	Chumphon, Thailand	P	F	42.4	11.3	12.8	5.2	1.5	2.9	2.7	4.7	3.9	3.5	1
ZMMU A-8057	Suan Phueng, Ratchaburi, Thailand	R	M	30.3	8.7	10.3	3.5	1.2	2	2	3.9	3.2	3.1	0.5
ZMMU A-8055	Suan Phueng, Ratchaburi, Thailand	R	M	35.7	11	12	4.5	1.4	2.3	2.9	4.3	3.6	3.4	0.8
ZMMU A-8020	Phuket, Thailand	R	M	32.6	9.9	10.9	5	1.4	2.1	2.2	4	3.5	3.5	0.9
ZMMU A-8049	Suan Phueng, Ratchaburi, Thailand	R	M	33.3	9.8	10.6	5	1.3	2.2	2.2	3.9	3.7	3.2	0.8
ZMMU A-8060	Suan Phueng, Ratchaburi, Thailand	R	M	34.4	10.4	12	5.3	1.4	2.2	2.5	4.3	3.8	3.4	0.8
ZMMU A-8210	Suan Phueng, Ratchaburi, Thailand	R	M	33.9	9.5	11.2	5.2	1	2.4	2.5	4	3.6	3.2	0.7
ZMMU A-8048	Suan Phueng, Ratchaburi, Thailand	R	M	33.8	10.2	10.8	4.5	1.1	2.1	2.2	4.4	3.6	3	0.8
ZMMU A-8050	Suan Phueng, Ratchaburi, Thailand	R	M	34.3	10.8	11.3	4.6	1.1	2.5	2.7	4.6	3.4	3	0.9
ZMMU A-8034	Chumphon, Thailand	P	M	34.1	9.4	11.6	4.2	1.2	2.1	2.2	4.1	3.4	3	0.8
ZMMU A-8039	Chumphon, Thailand	P	M	30.4	9.7	9.9	4.5	1.1	2.1	2	3.7	3.2	3.4	0.6
ZMMU A-8059	Suan Phueng, Ratchaburi, Thailand	R	M	32.6	9.8	10.7	4.6	1.2	2.1	2.2	4.4	3.1	3.3	0.7
ZMMU A-8054	Suan Phueng, Ratchaburi, Thailand	R	M	34	10.1	11.2	4.7	1.1	2.2	2.2	4.3	3.5	3.1	0.7
ZMMU A-8051	Suan Phueng, Ratchaburi, Thailand	R	M	30.8	8.8	9	3.5	1.1	2	2	3.8	3.1	3	0.5
ZMMU A-8047	Suan Phueng, Ratchaburi, Thailand	R	M	33.8	9.7	11.1	4.5	1.1	2.3	2.2	4.4	3.6	3.3	0.8
ZMMU A-8056	Suan Phueng, Ratchaburi, Thailand	R	M	33.4	9.6	10.6	4.9	1.4	2.2	2.4	4.3	3.6	3.2	0.8
ZMMU A-8058	Suan Phueng, Ratchaburi, Thailand	R	M	33.5	9.8	11.2	4.7	1.5	2.4	2.5	4.5	3.7	3.2	0.8
ZMMU A-8052	Suan Phueng, Ratchaburi, Thailand	R	M	31.8	9.6	10.7	4.7	1.2	2.2	2.5	4.3	3.7	3.2	0.8
ZMMU A-8053	Suan Phueng, Ratchaburi, Thailand	R	M	31.2	9.1	10.5	4.7	1.2	2.2	2.5	4.2	3.4	3.1	0.8

ZMMU ID	Sex	ESD	TD	CRL1	PGW	PGL	FLL	FHL	FAW	HAL	F1	F2	F3	F4	IMC
Ingerophrynus parvus															
ZMMU A-8029	F	5.2	4.3	7.7	3.5	4.6	31.6	24.5	3.6	12.5	5.8	4	7.7	2.5	1.9
ZMMU A-8021	F	4.8	3.2	6.9	3.9	3.8	33.3	24.6	4.3	12.5	7.5	4.1	8.9	3.5	1.3
ZMMU NAP-09684	F	5.2	3.7	7.8	2.9	3.8	31.2	23.5	3.4	11.8	6.6	3.8	7.9	2.7	0.9
ZMMU A-8025	M	4	2	6.1	2.4	3	23.2	17.5	3	8.6	4.8	2.2	5.6	1.8	1.4
ZMMU A-8026	M	4	1.9	6	2.4	2.3	24.2	17.9	3.8	8.7	4.5	2.9	6.3	2.2	0.7
ZMMU A-8024	M	4	2	6	2.4	3	23.3	18.3	3.6	9.5	4.9	3.4	7.2	2	0.9
ZMMU A-8022	M	3.4	2.1	6.3	2.6	2.4	23.7	18.4	3.2	9	4.5	2.8	6.3	1.6	0.8
ZMMU A-8023	M	3.7	2.5	6	2.5	2.9	23.4	18.2	3.1	8.6	4.6	3.5	7	2.3	1
ZMMU A-8027	M	3.8	2.2	6	2.5	2.3	25.5	19.1	3.6	9.5	4.6	3.5	6.5	2.1	1.4
ZMMU A-8028	M	4.2	2.4	6.1	2.4	2.8	26	18.9	3.9	9.9	4.9	3	6.5	2.2	1.2
Ingerophrynus chrysolophus **sp. nov.**															
ZMMU A-8035	F	3.9	2.5	5.9	2.6	2.7	24.2	18.6	2.1	9.2	4.5	3	6.4	2.1	1.3
ZMMU A-8030	F	4.4	2.7	5.7	2.9	2.7	22.1	17.7	2.6	8.7	4.6	2.6	5.8	2.2	1.1
ZMMU A-8036	F	3.8	2.4	4.4	2.5	2.4	22.2	17.4	2.9	8.5	4.8	2.7	5.6	2.1	1.1
ZMMU A-8037	F	3.8	3	4.7	2.6	2.6	22.5	16.8	3	8.3	4.6	2.9	5.6	1.9	1.1
ZMMU NAP-09425	F	3.8	3.7	5.7	2.7	4.4	25.3	19.4	3.5	9.4	3.3	4.7	5.8	2.3	1.3
ZMMU A-8211	F	3.6	2.3	5.2	2.6	5.2	24.9	19.5	2.7	9.3	3.9	3.1	6.3	2.6	1.2
ZMMU A-8061	F	4	2.5	6.5	3.9	3.9	23.3	18.8	2.7	9.8	5.4	3.7	7	2.1	1.5
ZMMU A-8031	F	4.4	2.7	5.9	2.8	2.6	27.9	20.9	2.9	9.9	5.1	4	7.5	2.3	1.4
ZMMU A-8033	F	4.3	2.6	5.6	3.3	3.6	27.5	20.6	3.2	10.1	5.4	3.7	6.6	2.3	1.4
ZMMU A-8032	F	4.5	2.4	5.9	3	3.5	28.7	22.2	2.9	10.4	6	4	7.1	2.6	1.5
ZMMU A-8057	M	3.7	2.3	5.7	2.4	2.6	20.4	16	2.7	7.7	4	2.2	5.6	1.6	0.9
ZMMU A-8055	M	3.9	2.5	6.3	3.7	3.8	21.3	17.4	3.7	8.7	4.1	2.7	5.7	2.1	1
ZMMU A-8020	M	3.8	2.3	5.3	2.9	2.8	20.8	16.8	3.4	8.7	4.8	2.3	5.8	1.9	1.2
ZMMU A-8049	M	3.8	2.5	5.6	2.5	2.9	22.2	16.3	3.2	8.6	4.7	2.6	5.7	2	1

ZMMU ID	Sex	ESD	TD	CRL1	PGW	PGL	FLL	FHL	FAW	HAL	F1	F2	F3	F4	IMC
ZMMU A-8060	M	3.9	2.6	6.1	3.1	3.1	22.7	17.4	3.4	8.7	4.5	2.7	5.9	1.9	1.1
ZMMU A-8210	M	3.6	2.1	5.7	2.5	3.7	21.3	17.7	2.2	8.9	3.9	2.7	5.7	2.1	0.9
ZMMU A-8048	M	3.9	2.4	5.9	2.6	3.6	22	17	3.3	8.9	4.4	2.8	6.5	1.9	1.4
ZMMU A-8050	M	3.6	2.8	5.3	2.6	3.2	22.2	18.2	3.5	9.4	4.3	2.9	5.2	2	1.4
ZMMU A-8034	M	3.8	2.4	5.1	3.2	3.1	23.8	18.3	3.1	8.8	4.1	2.8	6	1.8	1.2
ZMMU A-8039	M	3.5	2.2	5.3	2.2	2.7	22	16	2.8	7.5	3.8	2.7	5.3	2	1.2
ZMMU A-8059	M	3.4	2.4	5.3	2.4	3	23.7	17.6	3.3	8.7	4.3	2.7	6	2	1.1
ZMMU A-8054	M	3.5	2.3	5.6	2.4	3.6	23.9	18.1	2.8	8.6	4.2	2.9	6	2	1
ZMMU A-8051	M	3.6	2.2	5.3	2.5	2.6	20.7	16	2.6	7.8	4.1	2.2	5.2	1.7	0.9
ZMMU A-8047	M	3.9	2.4	5.9	2.7	2.9	22.6	17.4	3.3	8.9	4.4	2.8	6.4	1.8	1.4
ZMMU A-8056	M	3.9	2.6	5.7	3.1	2.8	22.4	17.2	3.1	8.6	4.6	2.7	5.8	1.9	1.2
ZMMU A-8058	M	3.9	2.5	5.8	3.2	3.4	22.3	17.4	3.4	8.7	4.6	2.5	5.9	1.9	1.2
ZMMU A-8052	M	3.8	2.6	5.7	3.2	3.1	22.4	17.5	3.1	8.9	4.7	2.6	5.9	1.9	1
ZMMU A-8053	M	3.7	2.4	5.5	2.7	2.5	20	16.1	3.2	7.7	3.9	2.6	5.2	1	1
ZMMU ID	**Sex**	**OMC**	**FEL**	**TIL**	**TFL**	**FOL**	**T1**	**T2**	**T3**	**T4**	**T5**	**IMT**	**OMT**	**CRL2**	
Ingerophrynus parvus															
ZMMU A-8029	F	3.2	21.2	21.5	28.4	16.5	4.9	2.8	4.4	7.8	2.2	2	1.4	3	
ZMMU A-8021	F	2.8	21.3	21.6	29	16.6	4.5	3	4.7	7.8	2	2.1	1.6	2.9	
ZMMU NAP-09684	F	2.3	19.8	20.7	29	16.9	4.9	4	6.2	8.9	2.5	1.9	1.7	3	
ZMMU A-8025	M	2.2	14.2	14.5	20	10.9	3.1	2	2.9	5.2	1.9	1.1	1.1	2	
ZMMU A-8026	M	1.9	15.1	14.5	21.6	11.7	3.1	2.3	3.3	6	1.9	1.4	1.1	2.6	
ZMMU A-8024	M	2	16.3	15.2	22.5	12.3	3.4	2.9	3.6	6	1.8	1.2	1.3	2	
ZMMU A-8022	M	2.1	14.3	14.8	20.9	11.8	2.4	2.2	4.1	5.4	1.5	1.2	1.1	1.9	
ZMMU A-8023	M	2	14.9	15.1	21.2	12.5	3.2	2.7	3.9	5.5	1.7	1.2	1.4	2	
ZMMU A-8027	M	2	16.3	15.3	22.4	12.7	3.5	2.1	3.4	6.3	1.8	1.8	1.4	1.9	
ZMMU A-8028	M	2.1	17	16.2	22.7	13.3	3.7	2.5	4.1	6.8	2	1.4	1.2	2.1	
Ingerophrynus chrysolophus **sp. nov.**															
ZMMU A-8035	F	1.8	14	14	21.8	13.1	3	2.6	3.4	6	1.8	1.1	1.1	2.3	
ZMMU A-8030	F	1.4	13.8	14.7	21.5	13	3.4	2.2	4.2	6.7	2	1.3	1.1	2.2	
ZMMU A-8036	F	1.9	13.5	13.8	21.1	12.5	3.3	2.2	3.6	6	1.9	1.3	1.3	2.2	
ZMMU A-8037	F	2	13.9	13.8	20.7	12	3	2.4	3.6	6.1	1.9	1.2	1.1	2	
ZMMU NAP-09425	F	2.2	14.6	15.9	23	15.2	4	2.8	3.9	6.3	2.1	1.4	1.3	2.7	
ZMMU A-8211	F	2.2	15.8	15	22.2	12.2	3.8	2	3.4	5.5	1.1	1.5	1.2	2.3	
ZMMU A-8061	F	2.1	15.2	14.5	21.5	13.1	4.2	2.4	3.6	6.6	1.9	1.3	1.3	2.5	
ZMMU A-8031	F	2.2	17.8	16.6	24.7	14.8	4	2.9	4.4	6.6	1.8	1.3	1.3	3.1	
ZMMU A-8033	F	2.1	16.3	16.3	24.3	14.4	3.5	2.6	4.2	7.5	1.8	1.4	1.4	2.4	
ZMMU A-8032	F	2.4	17.6	17.6	24.8	14.5	4.3	3	4.6	7.8	2.3	1.6	1.6	2.8	
ZMMU A-8057	M	1.7	14.3	12.1	18.6	11	3.2	2	3.3	5.3	1	1.2	1.2	2	
ZMMU A-8055	M	1.8	13.6	14.4	21	12.4	3.7	2.1	3.6	6.4	2.2	1.5	1.3	2.3	
ZMMU A-8020	M	1.8	13.3	13.5	20.7	12.2	3.4	2.7	3.6	6.5	1.8	1.4	1.4	1.9	
ZMMU A-8049	M	1.9	13.4	14.1	20.7	12	3.3	2.1	3.8	5.9	1.6	1.2	1.4	2.1	
ZMMU A-8060	M	1.9	13.6	13.7	20.7	12.2	3.5	2.3	3.8	6.3	1.6	1.2	1.1	2.1	
ZMMU A-8210	M	2.1	13.4	14	20	12.3	3.4	2.4	3.8	6.6	1.7	1.2	1	2.1	
ZMMU A-8048	M	2.2	13.5	14.5	20.8	12.5	3.9	2.3	3.8	5.4	1.6	1.4	1.1	1.9	
ZMMU A-8050	M	2	15.2	15.2	21.8	13.2	3.4	2.6	3.7	5.9	1.6	1.3	1.1	2.2	
ZMMU A-8034	M	2	14.2	14.5	21.6	13.3	4	2.6	3.3	5.5	1.5	1.3	1.3	2.5	
ZMMU A-8039	M	2	11.9	12.8	20.2	11.4	3.5	2.4	3.2	5.3	1.6	1.2	1.1	2	
ZMMU A-8059	M	1.9	15.1	14.6	21.8	12.6	3.3	2.4	3.8	5.8	1.6	1.3	1.3	1.9	
ZMMU A-8054	M	1.8	15.3	15	20.1	12.1	3.1	2.2	3.7	5.9	1.6	1.3	1.2	1.9	
ZMMU A-8051	M	1.8	13.3	12.9	18.8	11	3	2	3.3	5.3	1.5	1.2	1.1	1.8	
ZMMU A-8047	M	2	15	14.1	21.1	12.5	3.7	2.4	3.9	5.6	1.6	1.4	1.1	1.9	
ZMMU A-8056	M	1.9	14.2	14	20	11.9	3.3	2.1	3.8	6.3	1.7	1.2	1.1	1.9	
ZMMU A-8058	M	2	13.8	13.9	20.5	12.2	3.3	2.1	3.7	6.1	1.7	1.4	1.2	2.2	
ZMMU A-8052	M	1.9	13.9	13.9	20.5	12.4	3.1	2.2	3.9	6.3	1.6	1.1	1.1	2.1	
ZMMU A-8053	M	1.9	12.6	12.8	18.2	11	3.1	1.8	3.2	5	1.2	1.3	1.1	2.1	

The data were taken from the databases Worldclim 1 (https://www.worldclim.org), GlobCover 2009 (https://due.esrin.esa.int/page_globcover.php), Global Aridity and PET (https://csidotinfo.wordpress.com), and Percent tree coverage (https://github.com/globalmaps/gm_ve_v2). For convenience, each layer was abbreviated as follows: BIO1 = annual average temperature, BIO2 = daily average range (monthly average (maximum temperature - minimum temperature)), BIO3 = isothermality (BIO2/BIO7) (×100), BIO4 = temperature seasonality (standard deviation × 100), BIO5 = maximum temperature of the warmest month, BIO6 = minimum temperature of the coldest month, BIO7 = annual temperature range (BIO5-BIO6), BIO8 = average temperature of the wettest quarter, BIO9 = average temperature of the driest quarter, BIO10 = average temperature of the warmest quarter, BIO11 = average temperature of the coldest quarter, BIO12 = annual precipitation, BIO13 = precipitation of the wettest month, BIO14 = precipitation of the driest month, BIO15 = seasonality of precipitation (coefficient of variation), BIO16 = precipitation of the wettest quarter, BIO17 = driest quarter precipitation, BIO18 = warmest quarter precipitation, BIO19 = coldest quarter precipitation, AridIndex = aridization index, Barren = soil

fertility, cultivated land cultivation, Elevation = altitude, Exposition = slope exposure, Slope = drainage angle, Slope 3 cells = watershed angle squared 3 × 3 cells, Mixed = mixed land cover, Homogeneity = homogeneity of land cover, Shrub = percentage of shrub cover, Herbaceous = percentage of grass cover, Dec-broad = deciduous broadleaf forest, Ever-broad = evergreen broadleaf forests, Ever-decid = deciduous-broadleaf forests. The program ENMTools 1.3 (Warren et al. 2010) was used to filter SDM data and exclude correlated variables.

Models were assessed by computing the area under the curve (AUC), which was used to estimate the relative contribution of variables for each model. The reliability of the model was evaluated based on the receiver operating characteristic curve for training and test data, as well as their AUC values. We used the random test percentage tool settings for statistical evaluation of the model, with 75% of the randomly selected localities used to set up the model and 25% of the points used to test it. A model with AUC test values greater than 0.75 was considered to be useful, and above 0.90, very good (Swets 1988; Elith 2002). The final maps were designed using the QGIS Desktop 3.28 software (QGIS Development Team 2021). The resulting distribution image obtained shows in colors the calculated probability that the conditions are favorable for the species to inhabit (red: a high probability of favorable conditions; shades of blue: unlikely conditions).

Bioacoustic analysis

Advertisement calls of two populations of the *Ingerophrynus parvus* species complex were recorded using a portable digital audio recorder, the Zoom H5 (ZOOM Corporation, Tokyo, Japan), in stereo mode with 48 kHz sampling frequency and 16-bit precision. The recordings were taken in Khao Kra Jom Mt., Suan Phueng, Ratchaburi, Thailand (locality 3, Fig. 1; on 10 February 2022 at 19.00 h and at 24 °C), and in Gunung Jerai Mt., Kedah, Peninsular Malaysia (on 30 January 2010 at 20.00 h and at 25 °C). The ambient temperature was measured at the calling site immediately after the audio recording with a digital thermometer, the KTJ TA218A Digital LCD Thermometer-Hydrometer. Males were observed calling from the banks of slow-flowing forest streams. Calls were analyzed using Raven Pro 1.6.5 (K. Lisa Yang Center for Conservation Bioacoustics at the Cornell Lab of Ornithology 2024).

Audio spectrograms were calculated with a fast Fourier transform (FFT) of 512 points, 90% overlap, and 135 Hz grid spacing, using the Hanning window. The terminology of call analysis and description using a call-centered approach (defining uninterrupted units as calls whenever they are separated by long silent intervals) follows Koehler et al. (2017). In total, we measured eight recordings of calls, including 188 calls from three males of the *I. parvus* species complex from two localities (Suppl. material 1: table S5). Due to the poor quality of the recordings, we were able to measure only eight temporal parameters of the calls: duration of call series, intervals between call series, number of calls per series, call duration, intervals between successive calls within series, duration of call rise (CRT) and call fall (CFT), number of pulses per call, and one power parameter of calls: peak frequency (Fpeak).

Skeletal morphology

To study the skeletal morphology of *Ingerophrynus* cf. *parvus* from western Thailand, we examined X-ray projections for two specimens: ZMMU A-8059 (adult male from Ratchaburi Province) and ZMMU A-8032 (adult female from Chumphon Province) and performed a detailed micro-CT scanning. The scans were performed on a SkyScan 1272 microtomograph (Bruker, Billerica, USA) equipped with a Hamamatsu L10101-67 source (Hamamatsu Photonics, Hamamatsu, Japan) and a Ximea xiRAY16 camera (Ximea GmbH, Münster, Germany) at the Biological Faculty of Moscow University. The specimens were scanned at a source voltage of 100 kV and a source current of 100 μA without an X-ray filter. The samples were rotated 360° around the vertical axis with a rotation step of 0.1, with 4 frames averaging. From the obtained X-ray projections, stacks of virtual cross sections through the specimens' skeletal structures were reconstructed with the software NRecon® (Bruker micro-CT, Kontich, Belgium). The resulting stack consisted of 3599 images with a 4504x4504 resolution and a 5.42 um pixel size. This stack of images was imported into the three-dimensional visualization software package Avizo 8.1 for subsequent processing and visualization of osteological traits. The obtained scans were deposited in MorphoSource (https://www.morphosource.org/concern/media/000771864). Osteological terminology followed Trueb (1973) and Pregil (1981).

Results

Phylogenetic inference from mtDNA data

Our mtDNA-based genealogy of the genus *Ingerophrynus* (Fig. 2) includes sequences of ten out of the 13 currently recognized nominal species of the genus (Suppl. material 1: table S2) with the exception of *I. kumquat*, *I. claviger*, and *I. philippinicus*. Notably, we provide genetic data for the species *I. quadriporcatus* for the first time. The resulting tree is based on the analyses of a continuous mtDNA fragment that includes the 12S rRNA, 16S rRNA, and ND1 gene sequences (with a total length of up to 4,479 bp). BI and ML phylogenetic analyses resulted in almost identical tree topologies, with the monophyly of the genus *Ingerophrynus* strongly supported in both analyses (100/1.0; hereafter, values correspond to the ML UFBS/BI PP values of nodal support, respectively; Fig. 2).

Our tree shows a topology that slightly differs from topologies in previous studies (Chan and Grismer 2019;

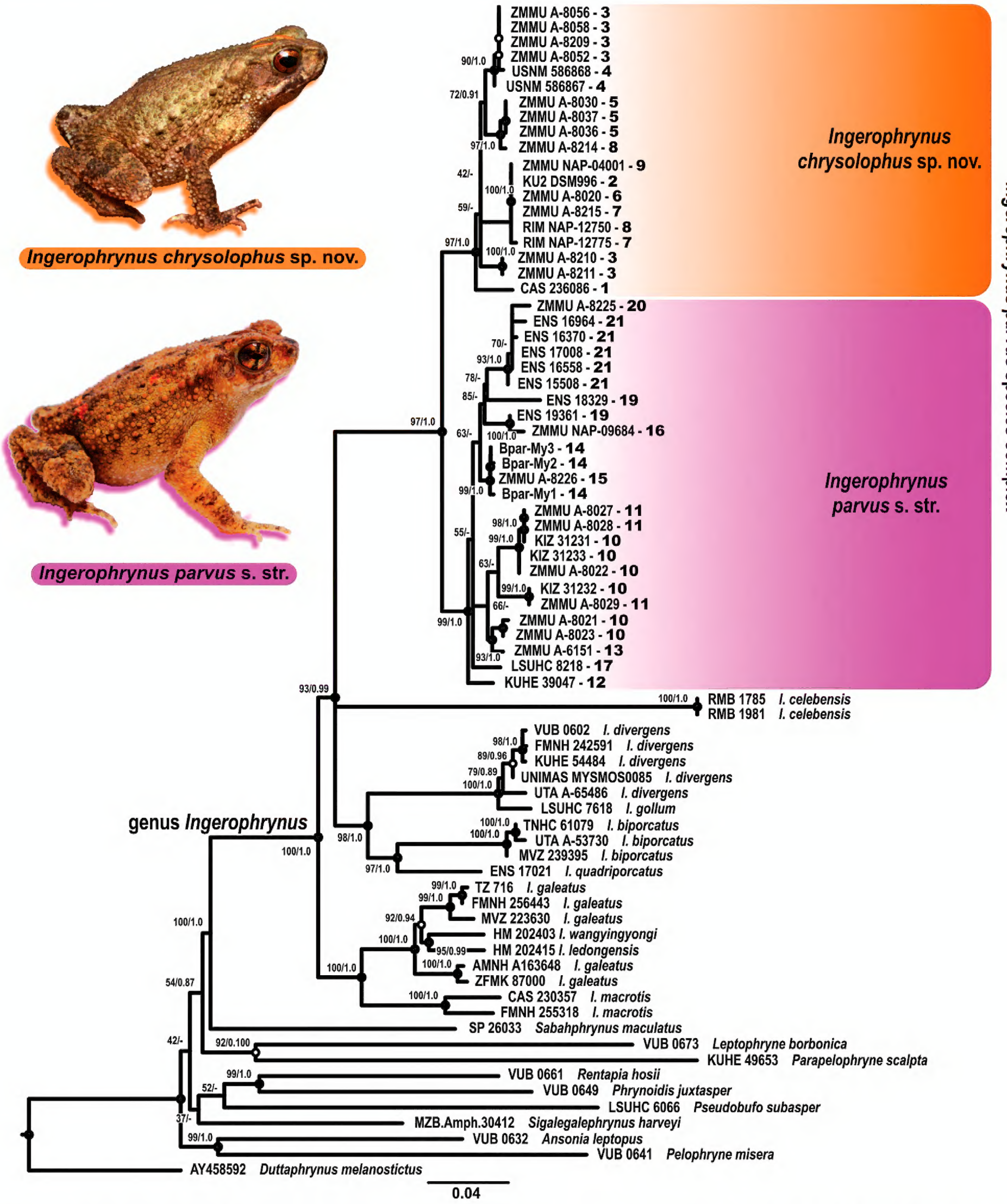

Figure 2. Phylogenetic relationships among the *Ingerophrynus parvus* species complex and other related *Ingerophrynus* species based on the mtDNA fragment including the 12S rRNA, 16S rRNA, and ND1 gene sequences (up to 4,479 bp). For voucher specimen information and GenBank accession numbers, see Suppl. material 1: table S2. Numbers at tree nodes correspond to ML UFBS/BI PP support values, respectively. Photographs by P. Pawangkhanant and N.A. Poyarkov.

Liu et al. 2025). According to our data (Fig. 2), the species of the genus *Ingerophrynus* form two reciprocally monophyletic groups: the Sunda clade (93/0.99) and the Indochinese clade (100/1.0). The Indochinese clade includes four species from mainland Southeast Asia and southern China—*I. galeatus*, *I. wangyingyongi*, *I. ledongensis*, and *I. macrotis*. Notably, *I. galeatus* was found to be paraphyletic with respect to *I. wangyingyongi* and *I. ledongensis*: the latter two species formed a clade (95/0.99) placed within the *I. galeatus* radiation with high nodal support (100/1.0). We also report deep divergence within *I. galeatus* and *I. macrotis* (Fig. 2), with uncorrected genetic *p*-distance in the 16S rRNA gene within these species reaching up to 2.95% and 3.44% of substitutions, respectively (Suppl. material 1:

table S6). At the same time, the level of divergence between *I. wangyingyongi* and *I. ledongensis* was minimal ($p = 2.21\%$; Suppl. material 1: table S6).

The remaining species form the Sunda clade, the monophyly of which is strongly supported by the BI analysis, while it receives only moderate levels of support in the ML analysis (93/0.99). The Sunda clade is comprised of three subclades, with the genealogical relationships between them remaining essentially unresolved (Fig. 2). The first subclade includes *I. biporcatus* + *I. quadriporcatus* from Indonesia (97/1.0) and *I. divergens* + *I. gollum* from Malaysia and Indonesia (100/1.0). It is notable that the sample of *I. gollum* appears to be genetically very close to *I. divergens* ($p = 2.32\%$; Suppl. material 1: table S6) and is reconstructed as its sister lineage, while the monophyly of *I. divergens* is not supported (79/0.89), and the species is comprised of several genetically divergent lineages. The second subclade is formed by a single species, *I. celebensis* (100/1.0), from Sulawesi Island of Indonesia. The third subclade is composed of the two reciprocally monophyletic lineages of the *I. parvus* species complex (97/1.0) (Fig. 2). The specimens from Sumatra, Peninsular Malaysia, and the southernmost Peninsular Thailand south of the Kangar-Pattani Line, identified here as *I. parvus* sensu stricto (hereafter, s. str.) (southern lineage), group with a significant nodal support (99/1.0), although the relationships within this group remain unresolved (55/-). The second group of *I.* cf. *parvus* is formed by the specimens from Peninsular Myanmar and Thailand north of the Kangar-Pattani Line (97/1.0) (northern lineage), and the relationships within this group are unresolved as well (59/-).

Genetic divergence in mtDNA markers

Pairwise uncorrected genetic *p*-distances were calculated based on the 465 bp-long fragment of the 16S rRNA mtDNA gene sequences among species of the genus *Ingerophrynus* and varied from 2.21% (between *I. wangyingyongi* and *I. ledongensis*) and 2.32% (between *I. gollum* and *I. divergens*) to 13.25% (between *I. celebensis* and *I. gollum*) (Suppl. material 1: table S6). The genetic divergence between the southern and northern lineages of the *I. parvus* species complex comprised 5.04% (between *Ingerophrynus* cf. *parvus* from Thailand and Myanmar and *I. parvus* **s. str.**). This 16S distance was notably higher than the proposed threshold of 3.0% for species-level divergence in anurans (Vieites et al. 2009), which was also recently supported as a criterion to delimit species based on instances of reproductive isolation (Dufresnes et al. 2021, 2023). We also report a high interspecific variation in several wide-ranging *Ingerophrynus* species, namely 0.98% among the populations of *I. divergens* (compared to an extremely low divergence of *I. gollum*: $p = 2.32\%$), *I. galeatus* ($p = 2.95\%$), and *I. macrotis* ($p = 3.44\%$). The intraspecific distances for *I.* cf. *parvus* from Thailand and Myanmar (northern lineage) and *I. parvus* **s. str**. (southern lineage) were 1.54% and 2.08%, respectively (Suppl. material 1: table S6).

Genetic differentiation according to nuDNA data

We sequenced three nuclear DNA genes (POMC, BDNF, and RAG1) for 16 specimens of the *Ingerophrynus parvus* species complex, with eight samples representing *I. parvus* **s. str.** and eight samples representing *I.* cf. *parvus* from Peninsular Thailand (Suppl. material 1: table S2). The analysis yielded five haplotypes of POMC, five haplotypes of BDNF, and seven haplotypes of RAG1 genes in the *I. parvus* species complex (Fig. 3). The resulting allele networks show clear separation between the nuclear gene haplotypes of the southern and northern lineages of the *I. parvus* species complex. The northern lineage of *I.* cf. *parvus* had two unique haplotypes of POMC and two unique haplotypes of RAG1 genes, which diverged from all other haplotypes observed in the southern lineage of *I. parvus* **s. str.** by seven and five mutation steps, respectively (Fig. 3A, C). Furthermore, the northern lineage of *I.* cf. *parvus* had two unique haplotypes of the *BDNF* gene, which were separated from the closest haplotype of the southern lineage of *I. parvus* **s. str.** by one to two mutational steps (Fig. 3B). These results support a significant evolutionary distinction between the northern and southern lineages of the *I. parvus* species complex.

Morphological differentiation

The morphological data on the *I. parvus* species complex was taken only from adult specimens in a good state of preservation and included measurements of 10 *Ingerophrynus parvus* **s. str.** from the southern lineage (seven males, three females) and 28 specimens of *I.* cf. *parvus* from the northern lineage (18 males, 10 females); all measurements are presented in Table 1. According to the box-and-whisker diagram illustrating the variability in body size between the sexes of the two lineages, females in the southern lineage of *I. parvus* **s. str.** were notably larger than in the northern lineage ($p < 0.005$), and sexual dimorphism in body size and proportions is seemingly more evident in the southern lineage than in the northern lineage of *I.* cf. *parvus* (Fig. 4). Principal Component Analysis (PCA) of 38 external morphological features showed complete separation of male specimens of the two lineages (Fig. 5). However, the percentage contributions of the first and second components (PCs) comprised 15.99% and 12.94% of the total variation, respectively, and were relatively small. Nevertheless, the specimens of each lineage formed distinct groups in the morphospace without overlapping (Fig. 5). Furthermore, we also analyzed qualitative external features, including coloration and the shape of cranial crests, which suggest morphological and chromatic distinctiveness of the two lineages. This data is given in the "Diagnosis" and "Coloration" sections of the new species description below. In addition, we obtained micro-CT scans of the skulls of male and female specimens of the northern lineage of *I.* cf. *parvus* and prepared a detailed craniological description.

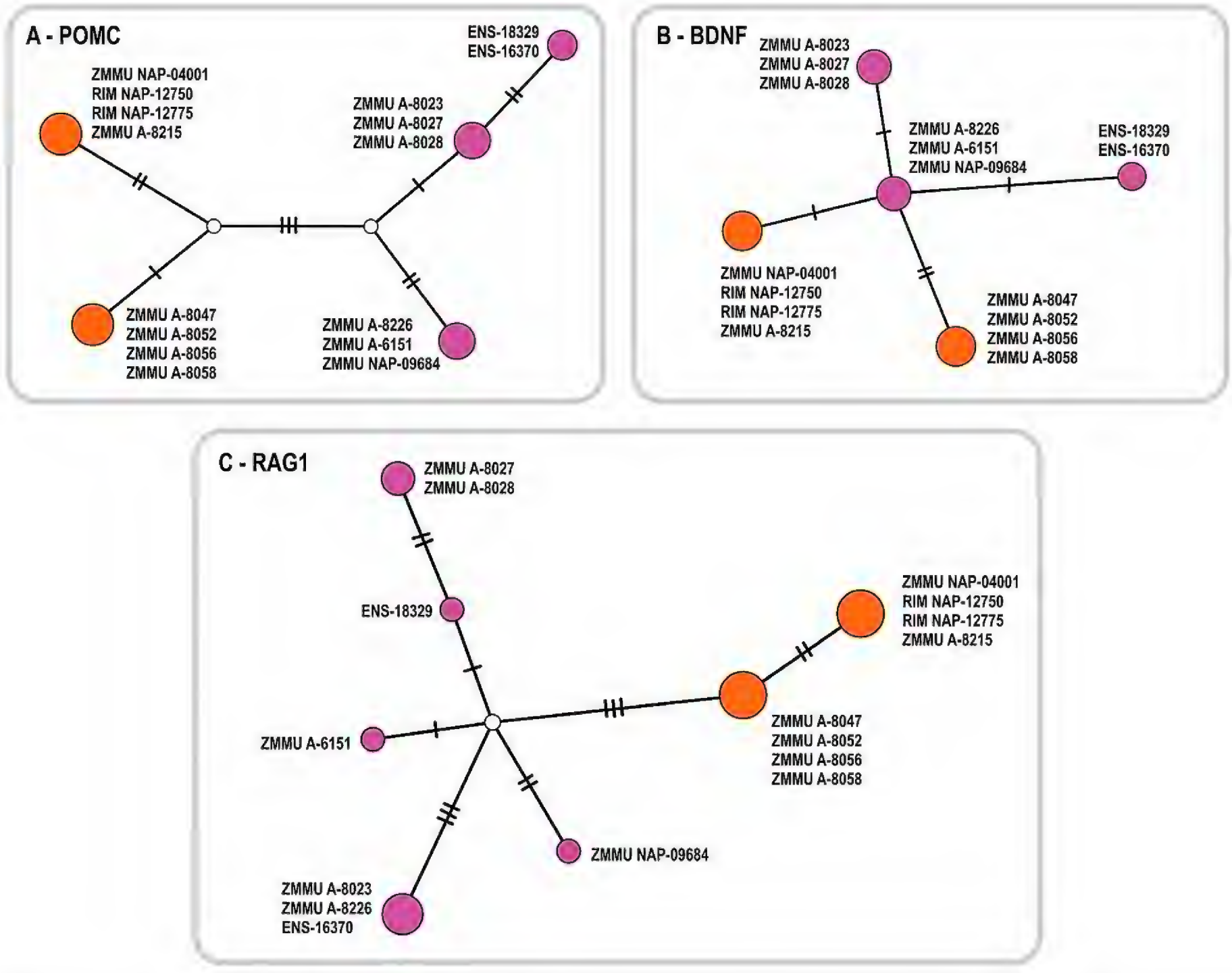

Figure 3. Nuclear allele median-joining network of POMC (**A.** 570 bp), BDNF (**B.** 672 bp), and RAG1 (**C.** 941 bp) nuclear gene haplotypes of the *Ingerophrynus parvus* species complex. Circle sizes are proportional to the number of samples/sequences; small open circles indicate hypothetical haplotypes (alleles); bars on branches correspond to the number of mutation steps. For voucher specimen information and GenBank accession numbers, see Suppl. material 1: table S2. Circle color corresponds to colors in Figs 1, 2, 4, 5.

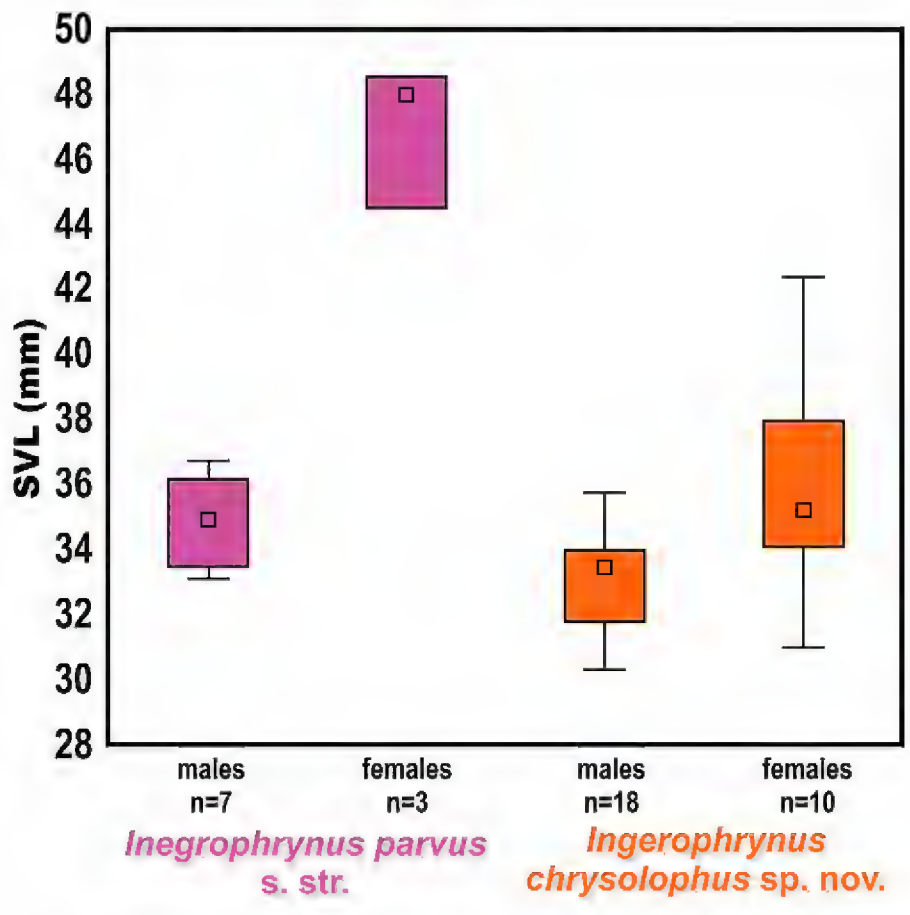

Figure 4. Boxplots of SVL (in mm) showing size variation among adult toads of the *Ingerophrynus parvus* species complex. Squares within each box represent the median, and boxes encompass the 75% and 25% quartiles; n indicates sample size. Box color corresponds to colors in Figs 1–3, 5.

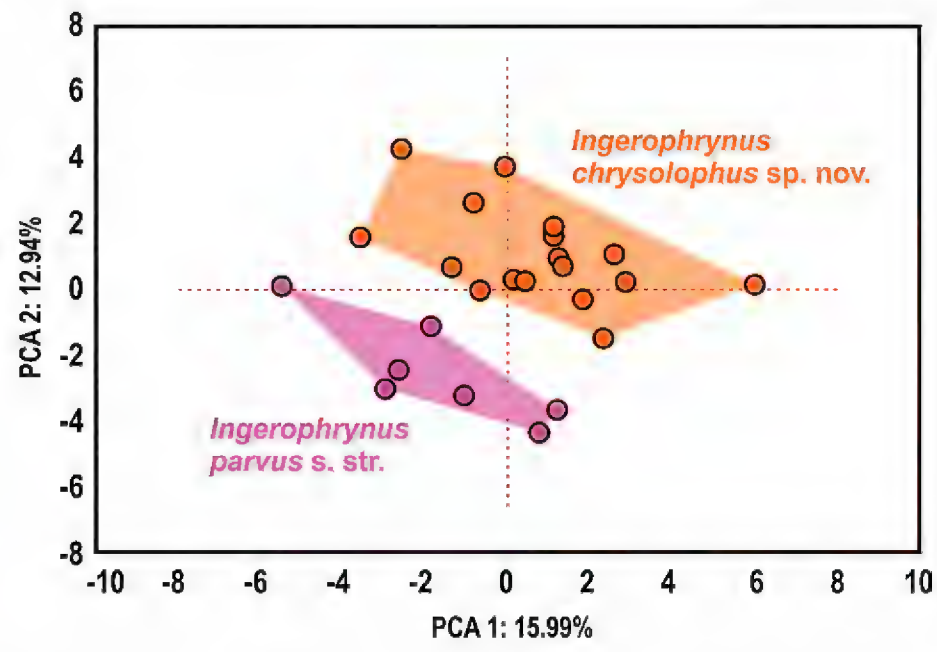

Figure 5. First and second factors of PCA based on analysis of 29 morphological characters measured in adult male specimens of the *Ingerophrynus parvus* species complex. Colors correspond to those in Figs 1–4.

Advertisement calls

The description of advertisement calls is based on recordings of three males from two populations: two males from Mt. Gunung Jerai, Kedah State, Peninsular Malaysia

(corresponding to the southern lineage of *Ingerophrynus parvus* **s. str.**; 87 calls measured), and one male from Mt. Khao Kra Jom, Suan Phueng District, Ratchaburi Province, Thailand (corresponding to the northern lineage of *I.* cf. *parvus*; 101 calls measured). The data on bioacoustic parameters of the advertisement calls of the two *I. parvus* species complex populations are presented in Suppl. material 1: table S5. In the description below, most numeral parameters are given as means ± SE, and the minimum and maximum values are given in parentheses (min–max). Time parameters are presented in seconds (s) and frequency parameters in hertz (Hz).

The male advertisement call of *I. parvus* s. str. (southern lineage; Fig. 6A) represents a series of high-pitched rising trills. The call series consisted of 13 to 15 calls emitted at a 0.6 ± 0.1 s (0.4–0.7 s) interval; a single call series lasted for 1.2 ± 0.1 s (1.1–1.2 s) on average. A single call series consisted of several calls (14.5 ± 0.8, 13–15) emitted at a 0.03 ± 0.004 s (0.02–0.03 s) interval. On average, a single call lasted for 0.06 ± 0.004 s (0.05–0.07 s). Each call consisted of 7.2 ± 0.9 (6–9) pulses. The call's amplitude increased slowly and reached a peak towards the end of the call, after which it gradually decreased (CRT = 0.04 ± 0.005 s, 0.03–0.05 s; CFT = 0.02 ± 0.004 s, 0.01–0.03 s; CRT/CFT = 2:1). The peak frequency of a call comprised 2,549 ± 93 Hz (2,438–2,625 Hz). The male advertisement call of *I. parvus* s. str. represents a series of noisy, high-pitched, rising trills that resemble the sound of a toy gun to the human ear.

The male advertisement call of *I.* cf. *parvus* (northern lineage; Fig. 6B) represents a series of high-pitched, frequent hooting. The call series consisted of eight to ten calls emitted at a 1.9 ± 0.1 s (1.8–2.0 s) interval; a single call series lasted for 1.1 ± 0.3 s (0.7–1.3 s) on average. A single call series consisted of several calls (9.4 ± 0.9, 8–10) emitted at a 0.1 ± 0.02 s (0.06–0.15 s) interval. On average, a single call lasted for 0.03 ± 0.004 s (0.02–0.05 s). Each call consisted of 5.4 ± 0.5 (5–6) pulses. The call's amplitude increased sharply at the beginning of a call, after which it gradually decreased (CRT = 0.01 ± 0.003 s, 0.01–0.02 s; CFT = 0.02 ± 0.004 s, 0.02–0.04 s; CRT/CFT = 1:2). The peak frequency of a call comprised 1,351 ± 40 Hz (1,292–1,378). The male advertisement call of *I.* cf. *parvus* represents a series of high-pitched, frequent hooting to the human ear superficially resembling a call of an orthopteran.

Species distribution modeling

SDM maps based on geolocation points of the *Ingerophrynus parvus* species complex are shown in Fig. 7. The climatic niche models for the two lineages within the species complex (Fig. 7) show good resolution and are statistically significant: the average performance of the MaxEnt SDMs for the replicate runs was estimated at AUC = 0.982; test data AUC = 0.980 for the northern lineage of *I.* cf. *parvus* from Thailand, Myanmar, and Cambodia; and training data AUC = 0.986 ans test data AUC = 0.956 for the southern lineage of *I. parvus* s. str. Variables that primarily account for species presence for the northern lineage of *I.* cf. *parvus* include isothermality (Bio 03), precipitation of the driest month (Bio 14), temperature seasonality (Bio 04), and coldest quarter precipitation (Bio 19). Variables that primarily account for species presence for the southern lineage of *I. parvus* s. str. include precipitation of the driest month (Bio 14), slope/watershed angle squared 3 × 3 (Slo 3), average temperature of the driest quarter (Bio 09), and annual temperature range (Bio 07). The climatic niche models also demonstrate almost complete non-overlapping of the niches of the two lineages, with the boundary between them generally corresponding to the Kangar-Pattani Line (Fig. 7), widely recognized as the zone of turnover between seasonal monsoon forests and humid equatorial forests (Poyarkov et al. 2021, 2023). Therefore, the northern lineage of *I.* cf. *parvus* from Thailand, Myanmar, and Cambodia inhabits tropical and subequatorial mountain forests with a more pronounced seasonality than the southern lineage of *I. parvus* s. str., which is restricted to equatorial perhumid forests.

Systematics

Bufo parvus was described by Boulenger (1887) based on 15 syntype specimens collected "within a radius of fifty miles from the town of Malacca," Malaysia (see locality 18; Fig. 1). Several subsequent studies reported this species from the Seribuat Archipelago of Malaysia (Grismer 2012); Sumatra (Manthey and Grossmann 1997; Iskandar 1998); southern and western Thailand (Taylor 1962; Srion et al. 2018); eastern Thailand (Chan-ard et al. 2011; Niyomwan et al. 2019); western Cambodia (Ohler et al. 2002; Neang and Holden 2008; Holden 2023); and southeastern Myanmar (Mulcahy et al. 2018; Zug and Mulcahy 2020; Zug 2022). Based on morphological data, Inger (1966) suggested that *Bufo* (now *Ingerophrynus*) *parvus* might represent a subspecies of *I. biporcatus*; later, Inger (1972) placed this taxon in the *Bufo* (now *Ingerophrynus*) *biporcatus* species group as a distinct species.

Several previous studies hinted at the existence of hidden diversity within *I. parvus*. Srion et al. (2018) reported on significant morphological divergence among populations in peninsular Thailand but refrained from any taxonomic conclusions. More recently, Chan and Grismer (2019), based on the analysis of 16S rRNA mtDNA fragments, suggested that *I. parvus* actually represents a species complex but again did not discuss its taxonomy in detail. In this study, we present an integrative taxonomic analysis of the *I. parvus* species complex based on the analyses of mtDNA and nuDNA genetic markers, external morphology, osteology, bioacoustics, and species distribution modeling. Our phylogenetic analysis suggested that *I. parvus* includes two major lineages: the southern lineage, distributed from southernmost Peninsular Thailand to Peninsular Malaysia and Sumatra, and the northern lineage, distributed across Peninsular Thailand

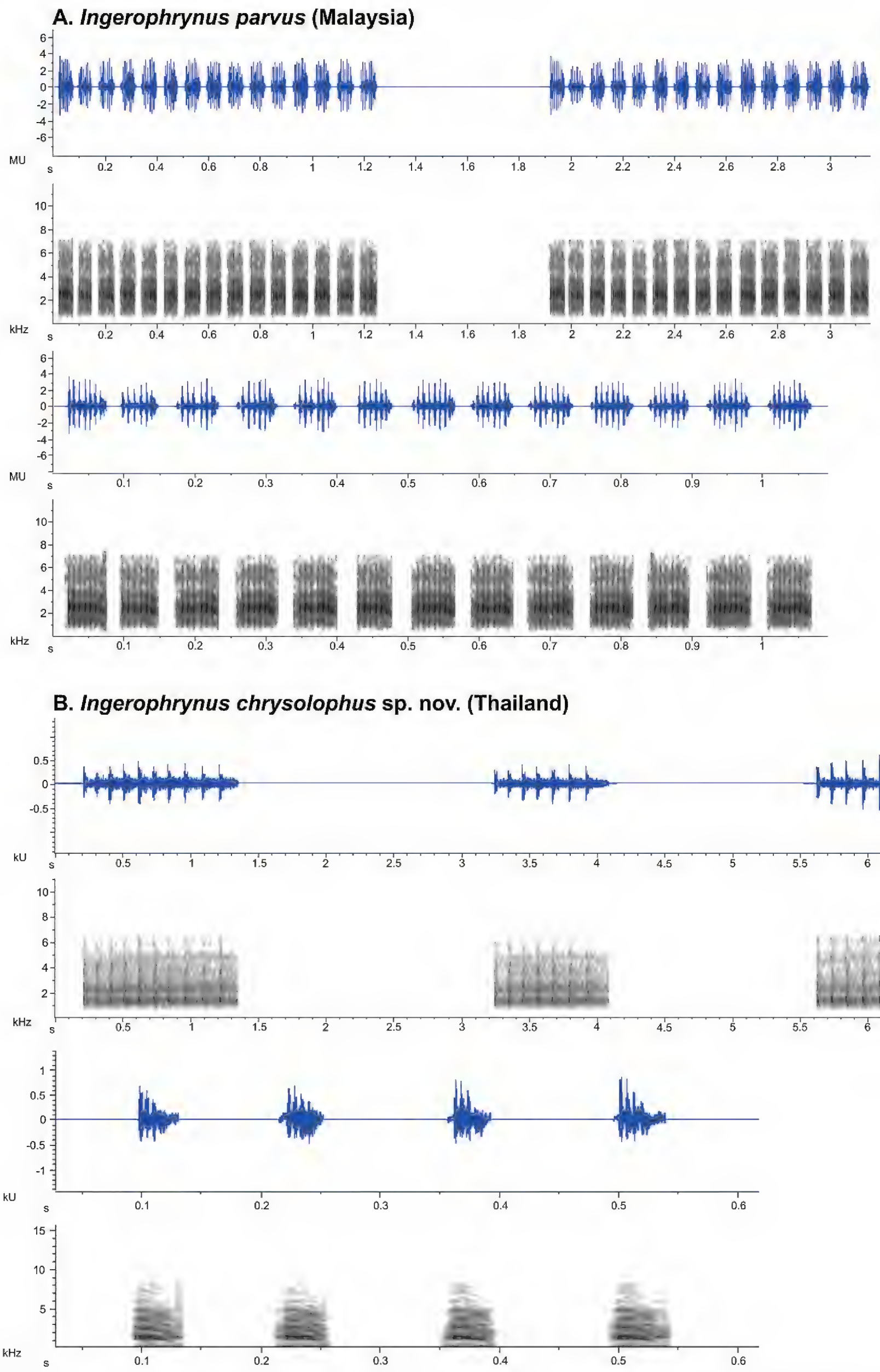

Figure 6. The call of *Ingerophrynus. parvus* s. str. from Selangor, Malaysia (**A**) and *Ingerophrynus chrysolophus* sp. nov. (**B**) from Chumphon, Thailand. **A.** 3 s waveform of relative amplitude (Rel. amp.) and corresponding spectrogram over time (above); 1 s waveform of relative amplitude (Rel. amp.) and corresponding spectrogram over time, obtained from the last two calls in **A** (below); **B.** 6.5 s waveform of relative amplitude (Rel. amp.) and corresponding spectrogram over time (above); 0.6 s waveform of relative amplitude (Rel. amp.) and corresponding spectrogram over time, obtained from the last two calls in **B** (below). Data on acoustic characters are summarized in Suppl. material 1: table S6.

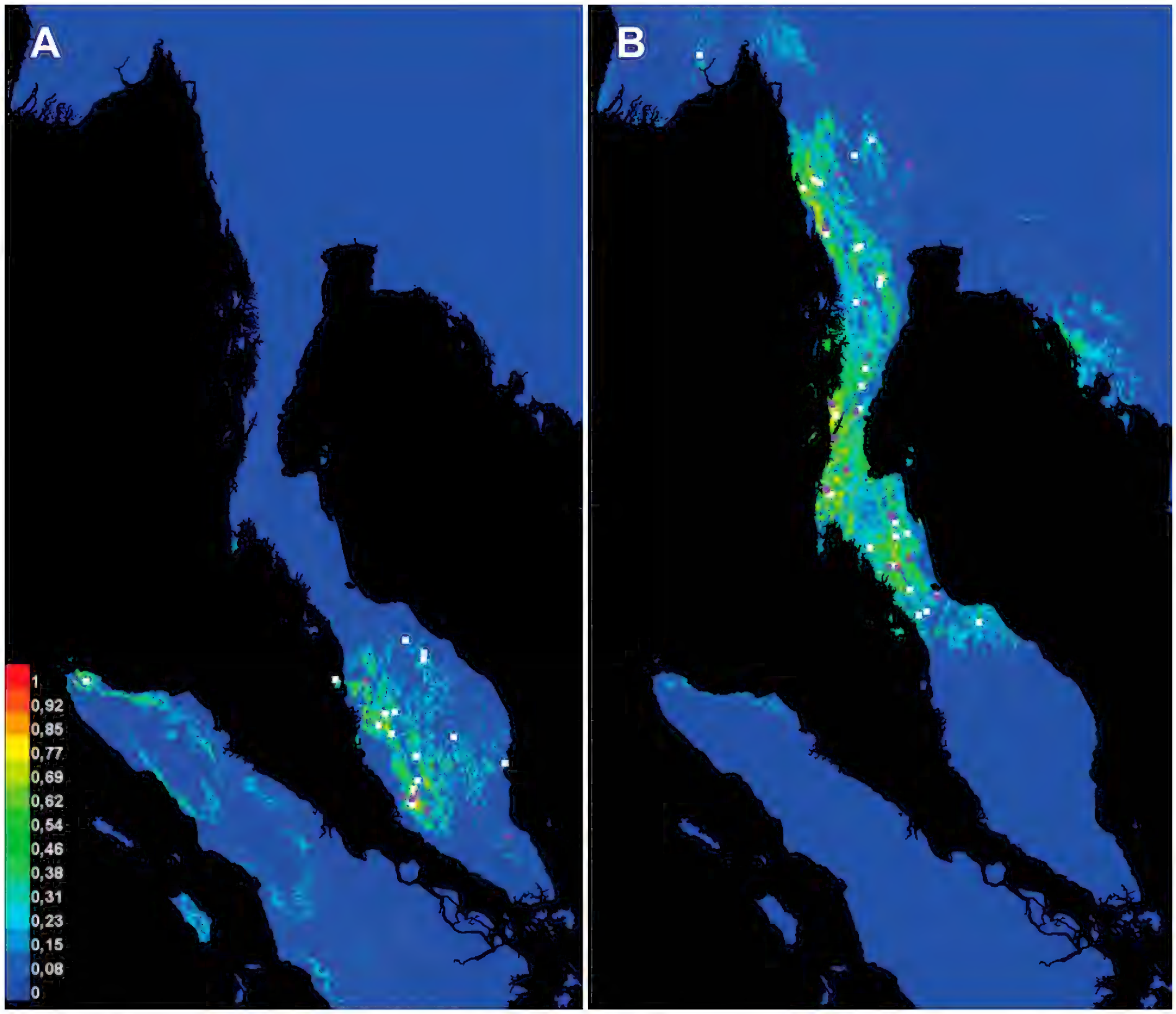

Figure 7. Climatic models of ranges of *Ingerophrynus parvus* s. str. (**A**) and *Ingerophrynus chrysolophus* sp. nov. (**B**) built in MaxEnt. Red to green indicates a high probability of suitable conditions for the species; shades of blue indicate less suitable conditions. White dots correspond to known localities for both species (see Suppl. material 1: table S5 for details on locality information and data sources).

and Myanmar to eastern Thailand and western Cambodia (Fig. 1). In mitochondrial genealogy, the two lineages are unambiguously reconstructed as sister lineages (Fig. 2) with a significant genetic differentiation between them (5.04% for the 16S rRNA gene). Besides the robustly supported mitochondrial divergence, allele networks of three nuDNA genes (Fig. 3) suggest complete separation of the haplotypes of the southern and northern lineages of *I. parvus*. Furthermore, the distribution of the two lineages is likely parapatric with almost non-overlapping climatic niche models, as suggested by the SDM analysis (Fig. 7); the ranges of the southern and northern lineages of *I. parvus* are separated by the Kangar-Pattani, an important biogeographic barrier in Southeast Asia, which separates the evergreen equatorial montane forests from seasonal tropical and subequatorial forests (Fig. 1).

The examination of external morphology revealed several diagnostic differences between specimens from the northern and southern lineages of *I. parvus*. We further report on a number of diagnostically important characters in skull morphology and coloration that readily distinguish populations of the northern lineage of *I.* cf. *parvus* from the southern lineage of *I. parvus* s. str. and all other congeners (see the Morphological Differentiation section above and the Comparisons section below). Finally, the bioacoustic analysis, even though based on the limited number of calls analyzed, indicated stable differences in temporal and frequency parameters among the male advertisement calls of northern and southern lineages of *I. parvus*, which further underlines the evolutionary distinctiveness of these lineages.

From an evolutionary perspective, based on the cumulative molecular, bioacoustic, and morphological evidence (see Comparisons below; Figs 4, 5), we hypothesize that the two lineages of the *I. parvus* complex should be considered two independently evolving and discretely diagnosable evolutionary entities that should warrant taxonomic recognition. The type locality of *Bufo parvus* Boulenger,

1887, in "Malacca," Malaysia (Fig. 1), is located within the range of the southern lineage of *I. parvus*, while there are no available nomina associated with the northern lineage of the complex. Therefore, the northern populations of the *I. parvus* complex represent a yet unnamed independently evolving entity distinct from *I. parvus* s. str., which we formally describe below as a new species.

Ingerophrynus chrysolophus Arkhipov, Pawangkhanant, Sarker, Nguyen, Suwannapoom, Smith & Poyarkov, sp. nov.

https://zoobank.org/247A9AF5-A249-41B9-8A89-11133C0E4E66

Figs 1, 2, 8–11, Table 1

Chresonymy. *Ingerophrynus parvus* [partim] — Taylor (1962: 329–332); Ohler et al. (2002: 467); Neang and Holden (2008: 53); Chan-ard et al. (2011: 32–33); Mulcahy et al. (2018: 85–162); Srion et al. (2018: 1–7); Chan and Grismer (2019: 3); Niyomwan et al. (2019: 186–187); Zug and Mulcahy (2020: 29); Poyarkov et al. (2021: 20); Zug (2022: 15); Holden (2023: 63).

Type materials. ***Holotype.*** • ZMMU A-8030 (field label NAP-11571), adult female from Wat Tham Sanook Temple, Tha Sae District, Chumphon Province, Thailand (10.481°N, 99.073°E; elevation 65 m asl.), collected on 27 January 2022, by N.A. Poyarkov, D.V. Arkhipov, P. Pawangkhanant, and C. Suwannapoom.

Paratypes (n = 8). • ZMMU A-8034, A-8039 (two adult males; field labels NAP-11575, NAP-11580), and ZMMU A-8031–A-8033, A-8035–A-8037 (six adult females; field labels NAP-11572–11574, NAP-11576–11578) from Wat Tham Sanook Temple, Tha Sae District, Chumphon Province, Thailand (10.481°N, 99.073°E; elevation 65 m asl.), collected on 27 January 2022, by N.A. Poyarkov, D.V. Arkhipov, P. Pawangkhanant, and C. Suwannapoom.

Referred specimens (n = 16). • ZMMU A-8020 (adult male; field label NAP-11165) from Pa Klok District, Phuket Province, Thailand (8.039°N, 98.391°E; elevation 68 m asl.), collected on 15 January 2022, by N.A. Poyarkov, D.V. Arkhipov, P. Pawangkhanant, and C. Suwannapoom; • ZMMU A-8047–A-8060 (14 adult males; field labels NAP-11726–11740) and ZMMU A-8061 (adult female; field label NAP-11741) from Khao Kra Jom, Suan Phueng District, Ratchaburi Province, Thailand (13.582°N, 99.178°E; elevation 998 m asl.), collected on 30 January 2022, by N.A. Poyarkov, D.V. Arkhipov, P. Pawangkhanant, and C. Suwannapoom.

Diagnosis. A member of the genus *Ingerophrynus* with the following combination of morphological characters: a medium-sized species (SVL 30.3–35.7 mm in males, 34.0–42.4 mm in females); head large and wide (HL/HW 0.81–0.98 in males, 0.80–0.96 in females); parotoid elongate, narrow, and sharply raised; parotoid not continuous with an oblique row of conspicuously enlarged warts; warts on flanks less elevated than those of dorsum; cranial crests not thickened behind eyes; lores vertical; tympanum distinct, its diameter slightly exceeding two-thirds of eye length (TD/ED 0.53–0.64 in males, 0.51–0.77 in females); tibia relatively short (TIL/SVL 0.40–0.44 in males, 0.39–0.43 in females); males with a subgular vocal sac; no tarsal ridge or tibial gland; first finger longer than second; tip of third toe not reaching median subarticular tubercle of fourth toe; subarticular tubercles not enlarged; tarsal spine bases small; nuptial pads present; venter with low warts; ground color of flanks and dorsum light brown; dark brown stripes along the midline of the back; cranial ridges well-developed, bright orange.

Description of holotype (Fig. 8). Adult female in a good state of preservation, body stout (SVL 42.4 mm); head relatively large, wider than long (HL/HW 0.88); head with a pair of straight, cranial crests not thick, diverging and raised posteriorly (Fig. 8D); snout projecting beyond lower jaw, gently rounded in lateral view (Fig. 8C), truncated in dorsal view (Fig. 8D); upper eyelid lacking supraciliary tubercles; protuberant nostrils at tip of snout with lateral orientation; canthus rostralis sharp, lores vertical (Fig. 8C); tympanum distinct, approximately half diameter of eye (TD/ED 0.51); paratoid gland elongate, rounded, low in profile, separated from eyelid by supratympanic crest (Fig. 8D); obliquely oriented row of enlarged, round to elongate dorsolateral warts extend posteriorly from paratoid gland approximately two-thirds way down flanks (Fig. 8A).

Forelimbs relatively long and slender (28.7 mm), fingers moderately long, tips blunt, not swollen; relative finger lengths: II<I<IV<III; fingers free of webbing (Fig. 8E); finger subarticular tubercles distinct, conical; finger subarticular tubercle formula 1:1:2:1; inner metacarpal tubercle slightly elongate; outer metacarpal tubercle triangular-shaped, dilated, bigger than inner metacarpal tubercle (IMC/OMC 0.63); two metacarpal tubercles not in touch with each other (Fig. 8E). Hindlimbs robust and short; tibia relatively short (TIL/SVL 0.42); relative toe lengths: IV<II<I<III<IV; tips of toes like those of fingers; fourth toe nearly three times the length of third and fifth; third and fifth toes with nearly two phalanges free of web; fourth toe with four free phalanges; second toe nearly completely webbed; first toe completely webbed; webbing formula: I1-1½II1½-2½III2½-3IV3-2V; subarticular tubercles conspicuous, somewhat conical, much smaller than metatarsal tubercles, toe subarticular tubercle formula 1:1:2:3:1; inner metatarsal tubercle oval, shorter than length of first toe (IMT/T1 0.37); outer metatarsal tubercle smaller, rounded (Fig. 8F).

Skin on flanks and dorsum covered with numerous conical warts, those of flanks lower in profile than those of dorsum; warts of dorsum capped by numerous spinules; enlarged series of nearly symmetrical paravertebral warts on dorsum beginning posterior to orbit and extending posteriorly beyond sacrum; venter covered with coarsely spinose granules.

Coloration. In life (Fig. 9A), the overall ground color of the flanks and dorsum is light brown; a prominent, symmetrical pattern of stripes running along the midline of the back extends from the tip of the snout to just above the cloaca, fading slightly posteriorly (Fig. 8A); cranial

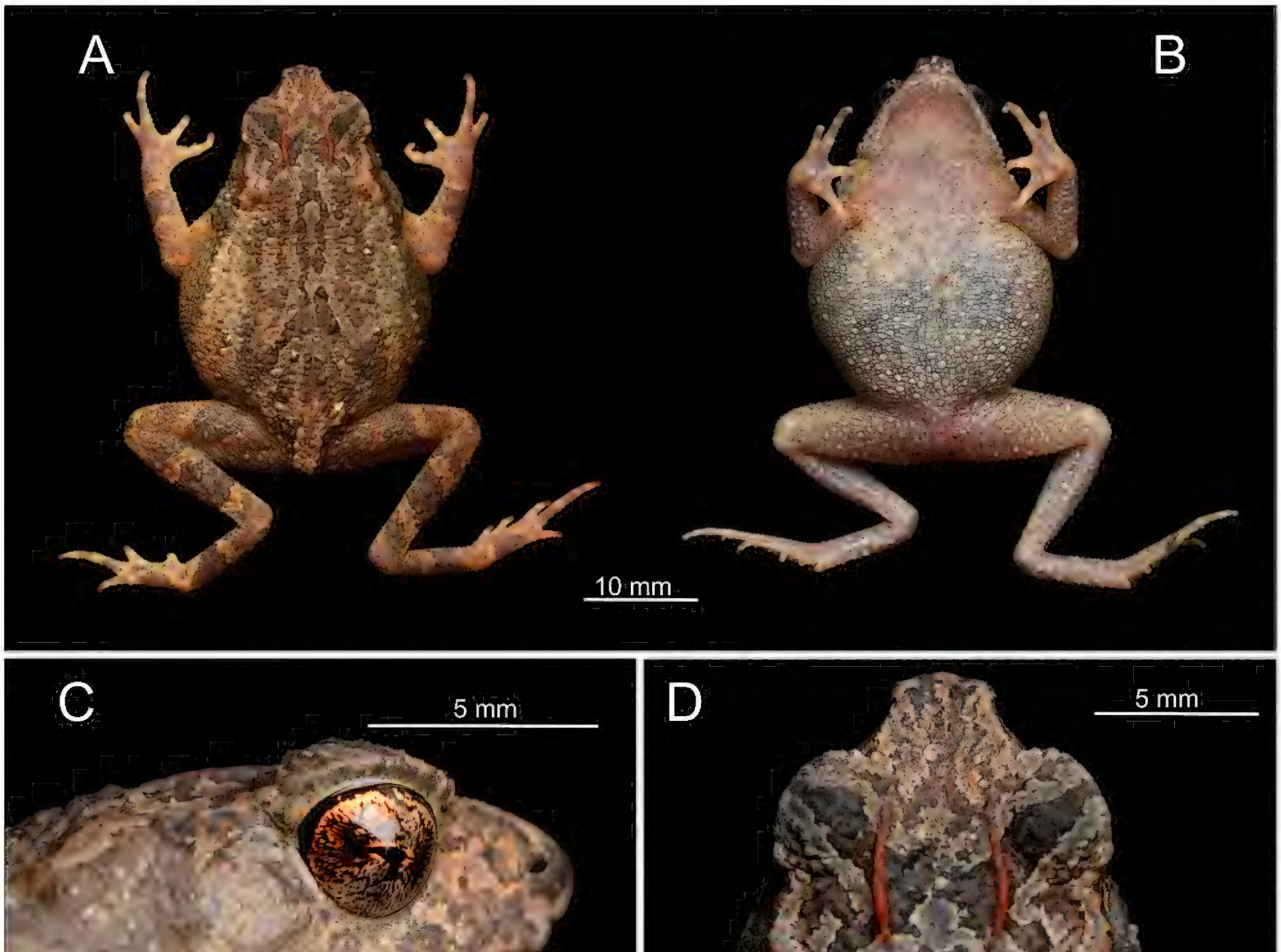

Figure 8. Holotype of *Ingerophrynus chrysolophus* sp. nov. from Wat Tham Sanook, Tha Sae, Chumphon, Thailand, in life—specimen ZMMU A-8030 (adult female). Dorsal aspect (**A**); ventral aspect (**B**); lateral view of head (**C**); dorsal view of head (**D**); volar view of the left hand (**E**); plantar view of the right foot (**F**). Photographs by N.A. Poyarkov. Scale bars: 5 mm.

ridges bright orange (Fig. 8C); parotoids and posteriorly extending dorsolateral warts dark beige, ventrally countershaded with dark brown (Fig. 9A), forming a border between the lighter brownish dorsum and dark brown flanks; dark brown crossbars on the limbs except for the brachia; the venter light brown to grayish, and ventral warts light beige (Fig. 8B). The pupil is horizontal and black, while the iris is also black, featuring dense golden reticulations on the dorsal and ventral sides and copper reticulations medially; the pupil is edged with a thin golden line (Fig. 8C). After preservation in ethanol for four years, all aspects of the color pattern remain; patterns

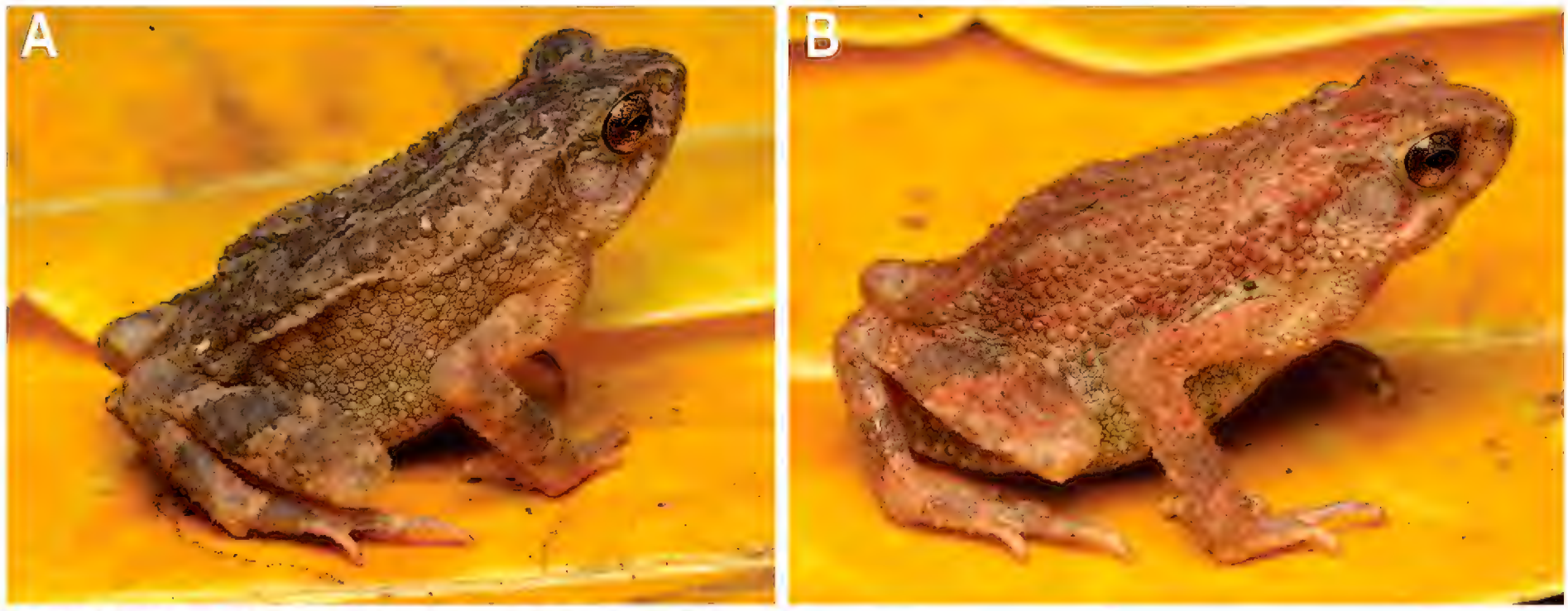

Figure 9. *Ingerophrynus chrysolophus* sp. nov. in life in situ. **A.** Holotype ZMMU A-8030 (adult female) from Wat Tham Sanook, Tha Sae, Chumphon, Thailand; **B.** Paratype ZMMU A-8034 (adult male) from Wat Tham Sanook, Tha Sae, Chumphon, Thailand; **C.** ZMMU A-8020 (adult male) from Pa Klok, Phuket, Thailand; **D.** ZMMU A-8059 (adult male) from Mt. Khao Kra Jom, Suan Phueng, Ratchaburi, Thailand. Photographs by N.A. Poyarkov.

of coloration of limbs and body are still visible but not as conspicuous as in life; bright orange colors on cranial crests and coloration of the iris completely faded.

Variation. The individuals in the type series and the referred specimens are all very similar in external appearance. Individual differences in size and body proportions are presented in Table 1. Males are significantly smaller than females ($p < 0.05$): mean male body length 33.0 ± 1.3 mm (SVL = 30.3–35.7 mm, n = 18); mean female body length 36.8 ± 2.2 mm (SVL = 34.0–42.4 mm; n = 10). Fig. 10 displays the variation in dorsal coloration of the paratypes. There were no significant differences in the coloration of male paratypes and females, except that males had a darker throat coloration. A female specimen, ZMMU A-8031, had a bright reddish-brown background dorsal coloration, markedly different from the duller brownish coloration of all other specimens examined (Fig. 10). There is a certain variation in the degree of development of dark dorsal markings among the individuals: females ZMMU A-8032, A-8035, and A-8036 had contrasting black blotches in scapular and sacral areas, while males ZMMU A-8034 and ZMMU A-8041 and female ZMMU A-8037 had almost no dark markings on the dorsum (Fig. 10). In general, males showed duller dorsal patterns with faint borders and less contrasting dark markings.

Tadpole morphology. A detailed description of the larval morphology of *Ingerophrynus chrysolophus* sp. nov. from Thailand was presented by Meewattana (2022: 30–31) (referred to as *I. parvus* in his work). Tadpoles of the new species have an oval-shaped head-body, 2/3 longer than wide; eyes with dorsal orientation; internarial distance comprising 2/3 of interorbital distance; spiracle sinistral; mouth-snout distance equal to snout-eye distance; vent median; tail broad with weak tail musculature; dorsal and ventral tail fins beginning at the tail base, both subequal in depth; and tail tip rounded (Meewattana 2022). Oral disc subterminal, with ventral orientation, small papillae in mouth corner, labial tooth row formula 2(2)/3; beaks black with serrated edges. Tadpoles reach 20.0–25.0 mm in length; the head-body is black in dorsal and lateral aspects and translucent in ventral aspect, with intestines being visible on the posterior half of the head-body length; tail muscles blackish, tail fins transparent (Meewattana 2022).

Figure 10. Variation in dorsal coloration of the paratypes and referred material of *Ingerophrynus chrysolophus* sp. nov. from Wat Tham Sanook, Tha Sae, Chumphon, Thailand, in life. Paratypes: adult male, ZMMU A-8034, ZMMU A-8039; adult female, ZMMU A-8031–8033, ZMMU A-8035–8037. Referred material: subadult topotypic males, ZMMU A-8038, RIM NAP-11589; subadult topotypic females, ZMMU A-8040–8044; subadults (sex not determined), ZMMU A-8045, ZMMU A-8046, RIM NAP-11591, RIM NAP-11593. Photographs by N.A. Poyarkov.

Osteological description. The following description of adult skull morphology is based on the tomographic data obtained for the adult male (ZMMU A-8059, paratype) and the adult female (ZMMU A-8032, paratype) (Fig. 11).

Cranium. Overall, the cranium of *Ingerophrynus chrysolophus* sp. nov. is generally well ossified; the highly tuberculous skin appears to be quite dense optically in this species and is visible in our reconstructions, concealing parts of the skull; the densest regions at the tip of the snout and on the upper eyelidswere cut off the scans; some elements on the cranial roof show traces of hyperossification, while the otic region seems underossified; the skull shape is almost triangular in dorsal (Fig. 11A, D) and ventral views (Fig. 11B, E) and close to trapezoid in lateral view (Fig. 11C, F). Snout distinctly truncate in dorsal (Fig. 11A, D) and ventral (Fig. 11B, E) views, not protruding beyond the upper jaw. The hyobranchial apparatus is mostly cartilaginous and thus invisible in our reconstruction; the only visible element is the well-ossified paired posteromedial process of the hyoid.

Premaxilla. The premaxilla is a paired bone, slightly arcuate dorsally, toothless (Fig. 11B, E). The premaxilla dorsally contributes to the internasal fontanelle (*cavum internasale*), ventrally contributes to the anteromedial fenestra, and dorsomedially contacts the ventromedial part of the external nares. The alary process of the premaxilla is oriented anterodorsally. The anterior surface of the premaxillary bones is slightly granular in female and smooth in male (Fig. 11B, E). The premaxilla contacts the maxillary bones posterolaterally and contributes to the anterior part of the nasal cavity.

Maxilla. The paired maxilla is a toothless bone, running laterally from the nasal capsule to the level of the otic region (Fig. 11B, E). The maxilla contacts the premaxillary anteriorly, the nasal dorsomedially, the palatine medially, the pterygoid posteromedially, and the quadratojugal posteriorly.

Nasal. The paired nasals form the dorsal part of the snout; they contact the maxillary ventrolaterally with the

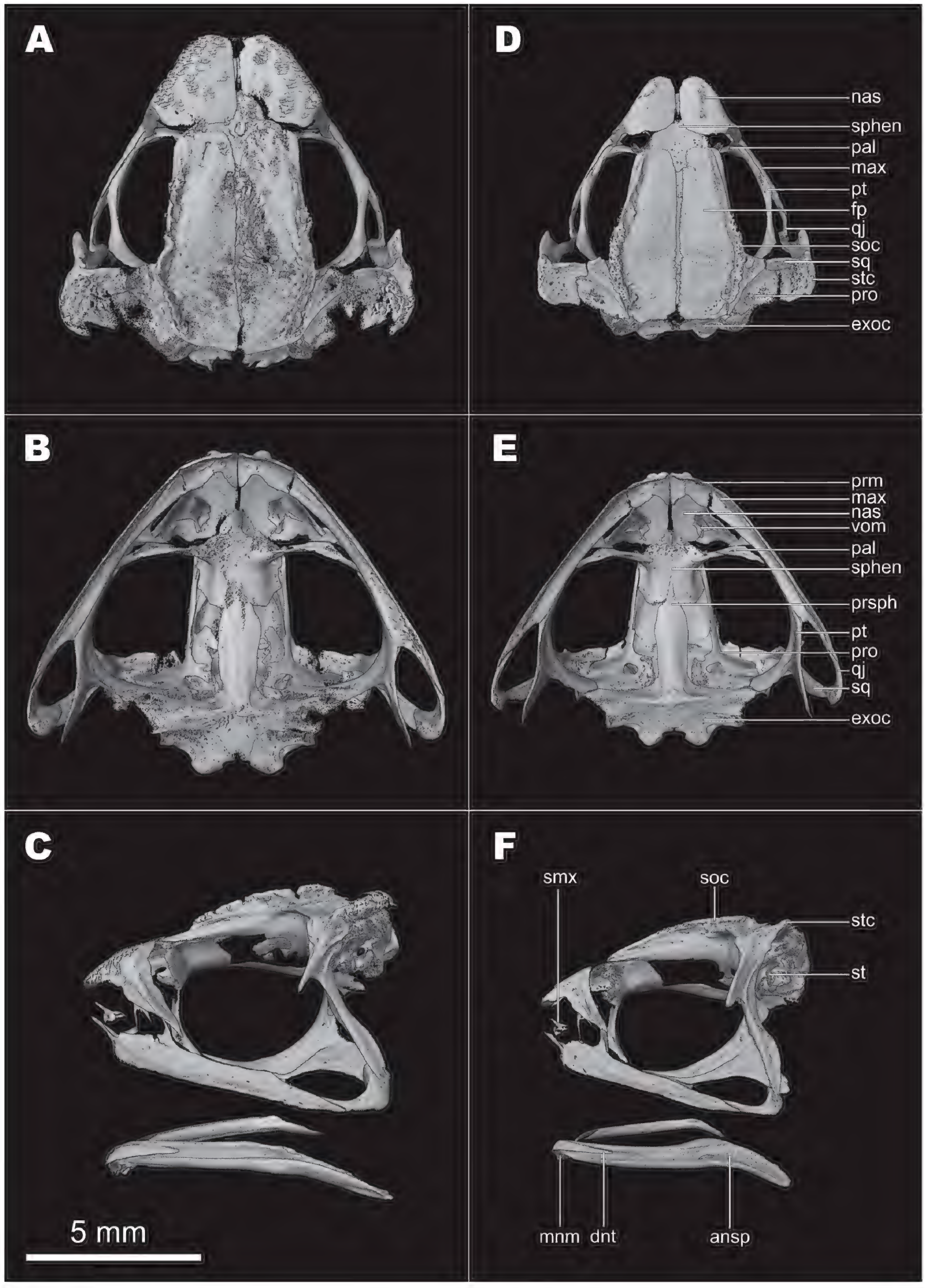

Figure 11. Cranial morphology of *Ingerophrynus chrysolophus* sp. nov.: adult female, paratype ZMMU A-8032 (**A–C**); adult male, paratype ZMMU A-8059 (**D–F**), visualized via micro-CT scanning. Skulls are shown in dorsal (**A, D**), ventral (**B, E**), and lateral (**C, F**) aspects. For the lateral views only, the left half of the cranium is shown. Abbreviations: nas – nasal, sphen – sphenethmoid, prsph – parasphenoid, prm – premaxilla, smx – septomaxilla, pal – palatine, vom – vomer, max – maxilla, pt – pterygoid, fp – frontoparietal, qj – quadratojugal, soc – supraorbital crest, sq – squamosal, stc – supratympanic crest, pro – prootic, exoc – exoccipital, st – stapes, mnm – mentomeckelian, dnt – dentary, ansp – angulosplenial. Visualization by D.V. Arkhipov and V.A. Gorin. Scale bar: 5 mm; all pictures are to scale.

well-pronounced maxillary process and the sphenethmoid posteriorly, which fills the space between the nasals and frontoparietals (Fig. 11A, C). The nasal contributes ventrally to the nasal cavity. Dorsal surfaces of nasal bones are depressed medially and overall are slightly shagreened in male and granular in female. The paired nasals are well separated from each other, forming an internasal fontanelle medially (Fig. 11A, D).

Frontoparietal. The large paired frontoparietals form the roof of the skull, separated by the frontoparietal suture across their length (Fig. 11A, D); they contact the sphenethmoid anteriorly and anteroventrally, the exooccipitals posteriorly, and the prootics posterodorsolaterally, and are fused with the latter posterolaterally. The dorsal surface of the frontoparietals is smooth in male and slightly granular in female. The dorsolateral parts of the frontoparietals form supraorbital crests all across their length and are granulated in the posterior half in male and along their entire length in female.

Septomaxilla. The paired septomaxilla is a small bone of a complex shape located in the anterior part of the snout (Fig. 11C, F). The septomaxilla contributes to the external nares and the anterior wall of the nasal cavity.

Vomer. The vomer is a rather small paired bone, triradiate in shape, located in the anterior part of the palatine region, covering the cranial base between the internal nares and bearing no teeth (Fig. 11B, E). A pair of vomers contributes to the medial and dorsal walls of the internal nares and to the ventral walls of nasal capsules.

Palatine. The paired palatine is a rod-shaped, toothless bone with a prominent ventral ridge (Fig. 11B, E). The palatine is located in the posterior part of the palatine region and contacts the sphenethmoid medially, the maxilla dorsolaterally, and the pterygoid posterolaterally.

Sphenethmoid. The sphenethmoid is a single bone subcylindrical in shape, forming the anterior portion of the neurocranium (Fig. 11B, E). It is structured like a typical cartilaginous bone with pronounced inner and outer bone layers. The sphenethmoid contacts the nasals anterodorsally, the frontoparietals posterodorsally, the palatines ventrolaterally, and the parasphenoid posteroventrally, and contributes to the nasal cavity anteriorly.

Parasphenoid. The single parasphenoid is a large sword-shaped bone plate forming the floor of the cranium (Fig. 11B, E). The parasphenoid contacts the sphenethmoid anteriorly, the prootics posterodorsally, the pterygoids posterolaterally, and the exoccipitals posteriorly. The parasphenoid is under-ossified laterally in the female specimen.

Squamosal. The paired hoe-shaped squamosals are located at the side of the cranium and at a right angle to the jaw arc (Fig. 11C, F). The squamosal contacts the prootic dorsomedially, the quadratojugal ventrally, and approaches the pterygoid medially. The squamosal is densely tuberculous dorsally, with the otic ramus forming the supratympanic crest on its dorsolateral surface (Fig. 11A, D). The medial part of the otic ramus appears to be underossified in the female specimen. Ventral and zygomatic rami are well developed, ossified, and smooth.

Pterygoid. The paired pterygoids are triradiate in shape, with each having three branches (rami; Fig. 11C, F). The *processus oticum* (medial ramus) is directed dorsomedially, with a prominent excavation in the posterior view, contacting the prootic. The *processus palatinum* (anterior ramus) is directed anteriorly, with a prominent lateral ridge, and contacts the maxilla laterally and the palatine anteriorly (Fig. 11B, E). The *processus quadratum* (posterior ramus) of the pterygoid is directed posteriorly, contacting the quadratojugal.

Quadratojugal. The paired quadratojugals are rather small bones, located posterolaterally on the skull (Fig. 11B, E). The quadratojugal contacts the maxilla anteriorly, the squamosal dorsally, approaching the pterygoid posteromedially, and articulating with the angulosplenial bone of the lower jaw posteroventrally.

Prootic. The prootic is an incompletely ossified paired bone, seemingly spongious, largely cartilaginous posteriorly (Fig. 11B, E). The posterolateral part of the dorsal surface of the prootic bears an excavation. The prootic contacts the squamosal dorsolaterally, the pterygoid ventrolaterally, the parasphenoid ventrally, and the frontoparietal dorsomedially and is fused with the latter anteromedially. The prootics largely contribute to the otic capsules.

Stapes. The paired stapes (columella) are largely mineralized, slightly arched, and extending medially (Fig. 11C, F). The stapes is oriented laterally and slightly anteriorly and comes close to the prootics, to the area of the oval window.

Saccular otoconia. The otic capsule is partially filled with calcium carbonate in the form of the saccular otoconia. The paired saccular otoconia are well mineralized, subspherical in shape, and located deep inside the inner ear.

Exoccipital. The paired exoccipital is the posteriormost bone of the skull, forming occipital condyles and the foramen magnum (Fig. 11B, E). The two exoccipitals slightly touch each other posterodorsally and posteroventrally. The exoccipitals show traces of underossification laterally, in the otic region. The exoccipital contacts the frontoparietal anterodorsally, the parasphenoid anteroventrally, and contributes anterolaterally to the otic capsule.

Mandible. The lower jaw is shaped like a solid bony arch and comprises three bone elements, namely, paired angulosplenials, dentaries, and mentomeckelians, the latter two being completely fused (Fig. 11C, F). The space between dentaries and angulosplenials is likely filled with Meckel's cartilage, invisible in our reconstructions.

Etymology. The species name "*chrysolophus*" is a Latinized adjective in the nominative singular, masculine gender, derived from the Ancient Greek words "*χρυσός*" or "*chrysos*," meaning "gold," and "*λόφος*" or "*lophos*," meaning "crest" or "ridge." The species name is given in reference to the characteristic golden-orange coloration of supratympanic crests in the new species. We suggest the following common names for the new species: Golden-crested Dwarf Toad (in English), Khang kok khrae hua tong (คางคกแคระหัวทอง, in Thai), and Zlatogrebnistaya shlemonosnaya zhaba (Златогребнистая шлемоносная жаба, in Russian).

Comparisons. *Ingerophrynus chrysolophus* sp. nov. can be distinguished from *I. biporcatus*, *I. celebensis*, *I. claviger*, *I. divergens*, *I. galeatus*, *I. ledongensis*, *I. macrotis*, *I. philippinicus*, *I. quadriporcatus*, and *I. wangyingyongi* by having small body size (SVL 30–36 mm in males, 34–42 mm in females vs. 55–70 mm in males, 60–80 mm in females of *I. biporcatus*; up to 130 mm of *I. celebensis*; 33 mm in male, 58–69 mm in females of *I. claviger*; 28–45 mm in males, 50–55 in females of *I. divergens*; up to 50 mm in males, 80 mm in females of *I. galeatus*; 47–55 in males, 62–64 mm in females of *I. ledongensis*; up to 50 mm in males, 55 mm in females of *I. macrotis*; 52–78 mm in males, 58–86 mm in females of *I. philippinicus*; 48–50 mm in males, 49–62 in females of *I. quadriporcatus*; and 44.8–53.3 mm in males, 54.3–57.9 mm in females of *I. wangyingyongi*). *Ingerophrynus chrysolophus* sp. nov. further differs from *I. biporcatus*, *I. divergens*, *I. galeatus*, *I. ledongensis*, *I. quadriporcatus*, and *I. wangyingyongi* by having parotoid not continuous with an oblique row of conspicuously enlarged warts (vs. continuous). *Ingerophrynus chrysolophus* sp. nov. can be further distinguished from *I. claviger* and *I. philippinicus* by having cranial crests not thickened behind eyes (vs. cranial crests distinctly thickened immediately behind the eye level). *Ingerophrynus chrysolophus* sp. nov. further differs from *I. kumquat* by having nuptial pads present (vs. absent) and by having first finger longer than second (vs. second finger longer than first).

Finally, *Ingerophrynus chrysolophus* sp. nov. superficially most closely resembles its sister species *I. parvus* s. str.; however, the new species can be readily distinguished from the latter by having the following suite of morphological characters: smaller body size in both sexes (SVL 30.3–35.7 mm [avg. 33.0 mm] in males, 34.0–42.4 mm [avg. 36.8 mm] in females vs. 33.1–36.7 mm [avg. 34.8 mm] in males, 44.5–48.5 mm [avg. 47.0 mm] in females); slightly higher HL/HW ratio in both sexes (0.81–0.98 [avg. 0.90] in males, 0.80–0.96 [avg. 0.87] in females vs. 0.83–0.89 [avg. 0.85] in males, 0.78–0.87 [avg. 0.83] in females); higher ratio TD/ED in males (0.53–0.64 [avg. 0.58] vs. 0.44–0.51 [avg. 0.48]), but lower in females (0.51–0.77 [avg. 0.60] vs. 0.53–0.81 [avg. 0.68]); lower ratio TIL/SVL in females (0.39–0.43 [avg. 0.41] vs. 0.44–0.45 [avg. 0.45]); lower ratio IMT/T1 in both sexes (0.33–0.42 [avg. 0.38] in males; 0.31–0.40 [avg. 0.37] in females vs. 0.35–0.51 [avg. 0.42] in males, 0.35–0.51 [avg. 0.42] in females), and by the presence of bright orange coloration of the cranial crests (vs. brown).

Advertisement call. The male advertisement call of *Ingerophrynus chrysolophus* sp. nov. is described in detail in the Results section (see above); the call parameters are presented in Suppl. material 1: table S5; the waveform and the sonogram of the male advertisement call of the new species are presented in Fig. 6B. The male advertisement call of the new species differs from the call of *I. parvus* s. str. by a lower peak frequency (1,292–1,378 Hz vs. 2,438–2,625 Hz), fewer short (0.02–0.05 s vs. 0.05–0.07 s) calls in the series (8–10 vs. 13–15), and by having fewer pulses in the call (5–6 vs. 6–9).

Distribution. *Ingerophrynus chrysolophus* sp. nov. is reliably known from central, eastern, western, and southern Thailand (Mae Hong Son, Tak, Kamphaeng Phet, Uthai Thani, Kanchanaburi, Ratchaburi, Phetchaburi, Prachuap Khiri Khan, Chumpon, Ranong, Surat Thani, Phang Nga, Phuket, Krabi, Nakhon Si Thamarat, Trang, Songkhla, Satun, Trat, and Chanthaburi provinces); the adjacent parts of southern Myanmar (Tanintharyi Region and Yangon State); and southwest Cambodia (Cardamom Mountains) (Fig. 1). According to the results of the species distribution modeling (Fig. 7B), the occurrence of the new species is expected in the northernmost Peninsular Malaysia (Perlis State); further studies are required to clarify the extent of its distribution in the Thai-Malay Peninsula.

Natural history notes. All individuals of the new species were collected during the night from swampy areas along the slow-moving, shallow stream within a closed-canopy evergreen montane or lowland tropical forest. Breeding and larval development take place in rain pools or side pools along the stream banks, typically with sandy or silty bottoms and numerous dead leaves and other plants accumulated on the bottom (Meewattana 2022). In Thailand, the new species occurs in various habitats, from undisturbed montane tropical forests to heavily disturbed bamboo forests and rubber plantations. In Suang Phueng (Ratchaburi Province), the new species was recorded in syntopy with three other bufonid species: *Ansonia karen* Suwannapoom, Grismer, Pawangkhanant, Naiduangchan, Yushchenko, Arkhipov, Wilkinson & Poyarkov, 2021; *Phrynoidis asper* (Gravenhorst, 1829); and *Duttaphrynus* cf. *melanostictus* (Schneider, 1799).

Conservation status. At present, the new species is known from multiple locations across southern, central, western, and eastern Thailand, southern Myanmar, and southwest Cambodia (Fig. 7B). The potential threats to this species are habitat loss and degradation due to intensified logging and deforestation. We propose the new species to be classified as Least Concern (LC) according to the IUCN's Red List categories (IUCN 2019).

Discussion

Our updated mtDNA-based genealogy is largely consistent with previous phylogenetic studies of the genus *Ingerophrynus* (Frost et al. 2006; Chan and Grismer 2019; Liu et al. 2025). The genus *Ingerophrynus* is confirmed as a monophyletic group, including two major clades: the Indochinese clade (*I. galeatus* + *I. macrotis*) and the Sundaland clade (all remaining species) (Fig. 2). In particular, we for the first time provide genetic data for *I. quadriporcatus*, which is recovered as a sister species of *I. biporcatus* (Fig. 2). The *I. parvus* species complex was found to be a member of the Sundaland clade of *Ingerophrynus* but is only distantly related to *I. biporcatus*, as hypothesized earlier (Inger 1966; Inger 1972). Furthermore, our phylogenetic reconstruction, coupled with genetic distances, indicates deep intraspecific diversification within such

wide-ranging complexes as *I. divergens* and *I. galeatus* (Fig. 2, Suppl. material 1: table S6), which requires further integrative taxonomic studies.

The taxonomy of the *Ingerophrynus galeatus* complex requires a special comment. Recently, Liu et al. (2025) revised this complex and described the population from Guangdong Province of China previously reported as *I. ledongensis* (Gong et al. 2011) as a new species, *I. wangyingyongi*. Liu et al. (2025) also demonstrated that *I. ledongensis* s. str. from Hainan Island of China is placed deeply within the radiation of the *I. galeatus* complex. In our mtDNA-based genealogy, *I. wangyingyongi* and *I. ledongensis* form a well-supported clade, rendering *I. galeatus* paraphyletic (Fig. 2). However, the study of Liu et al. (2025) contained several significant flaws, and their conclusions must be taken critically.

Firstly, just as in our study, Liu et al. (2025) demonstrated that *I. wangyingyongi* and *I. ledongensis* are placed within the radiation of *I. galeatus*; their position within the complex is essentially unresolved in the analysis of Liu et al. (2025), and their recognition makes *I. galeatus* paraphyletic. Nevertheless, Liu et al. (2025) labeled two lineages of *I. galeatus* as potential new species, *Ingerophrynus* sp. 1 (from Quang Binh, central Vietnam) and *Ingerophrynus* sp. 2 (from northern Vietnam), and referred to a lineage from Gia Lai (central Vietnam) as the true *I. galeatus* s. str. without providing any solid evidence for this decision. As the full species status of *I. wangyingyongi* and *I. ledongensis* is not evident, the fact that their placement within *I. galeatus* makes the latter species paraphyletic cannot be used as an argument for splitting the complex into several species, including two unnamed putative "species." A more conservative approach would suggest that *I. wangyingyongi* and *I. ledongensis* should be considered junior synonyms of *I. galeatus*, pending further molecular and morphological data on the remaining populations of the complex.

Secondly, the decision by Liu et al. (2025) to regard the Gia Lai population (central Vietnam) as nominotypical *I. galeatus* s. str. is questionable. Liu et al. (2025) refer to the type locality of *I. galeatus*, which was given by Günther (1864) as "Gamboja" (= Cambodia); the authors show it on the map as a locality in northern Cambodia (Liu et al. 2025: Fig. 5) and conclude that the population from the mountains of Gia Lai Province of Vietnam therefore belongs to *I. galeatus* s. str. due to its geographic proximity. Not only did Liu et al. (2025) not examine the type specimen *I. galeatus* (holotype NHMUK 1947.2.21.13), but their conclusion also appears to be erroneous. Stuart et al. (2006) demonstrated that *Bufo galeatus* was described by Günther (1864) from M. Henri Mouhot's Cambodian collection and that the type specimen of this species was almost certainly collected during Mouhot's expedition to "Brelum." Stuart et al. (2006) showed that this village was likely located on the present-day territory of Vietnam near the border with Cambodian Modulkiri Province (ca. 11°58'N, 107°12'E, in Binh Phuoc Province of Vietnam, according to Ashburton in Mouhot 1864). This area is located over 330 km southward from Gia Lai Province and belongs to the hilly foothills of the southern Annamites, an area biogeographically profoundly different from the montane forests of central Vietnam (Poyarkov et al. 2021, 2023). Therefore, the attribution of the Gia Lai population of the *I. galeatus* complex to *I. galeatus* s. str. by Liu et al. (2025) is unwarranted.

Finally, the level of genetic divergence between *I. wangyingyongi* and *I. ledongensis* in the 16S rRNA gene is minimal ($p = 2.21\%$; Suppl. material 1: table S6), and their divergence from the lineages of *I. galeatus* is also generally lower than $p = 3.0\%$, the formal level of species-level divergence in anurans (Vences et al. 2005; Vieites et al. 2009). In the absence of reliable diagnostic morphological characters, examination of the *I. galeatus* type specimen and sufficient samples of *I. galeatus*, and the lack of nuclear DNA or bioacoustic data, we conclude that such low divergence values in a single mtDNA marker are insufficient to justify the full species status of *I. wangyingyongi* and *I. ledongensis*. Recognizing the geographical and ecological specificity of the *I. galeatus* complex lineages from southern China, we follow the recommendations of Dufresnes et al. (2023, 2024) and therefore propose to treat them as subspecies *Ingerophrynus galeatus wangyingyongi* stat. nov. and *Ingerophrynus galeatus ledongensis* stat. nov. pending further integrative taxonomic analysis. Future studies should provide a comprehensive revision of the *I. galeatus* complex, including a meticulous analysis of its variation in nuDNA markers, as well as in morphological and bioacoustic characters. The taxonomic status of *I. gollum*, which was also found to be very closely related to *I. divergens* in 16S rRNA gene sequences ($p = 2.32\%$; Suppl. material 1: table S6), may also be reconsidered in the future; here we refrain from any taxonomic changes pending additional genetic and morphological data on the *I. divergens* complex.

It is also notable that Fei et al. (2012) assigned *I. ledongensis* to a separate genus, *Qiangbufo* Fei, Ye & Jiang, 2012. Our study, in accordance with the earlier results of Liu et al. (2025), places *I. galeatus ledongensis* stat. nov. deeply within the radiation of the genus *Ingerophrynus*, as one of the lineages of the *I. galeatus* complex. Therefore, our results confirm that *Qiangbufo* Fei, Ye & Jiang, 2012 should be regarded as a junior synonym of *Ingerophrynus* Frost, Grant, Faivovich, Bain, Haas, Haddad, de Sá, Channing, Wilkinson, Donnellan, Raxworthy, Campbell, Blotto, Moler, Drewes, Nussbaum, Lynch, Green & Wheeler, 2006, a taxonomy that is already widely accepted (Frost 2025). The nomen *Qiangbufo* is thus available for the mainland Asian clade of *Ingerophrynus* (including the *I. galeatus* complex and *I. macrotis*). However, further multilocus studies of *Ingerophrynus* are required to clarify the phylogenetic relationships of the genus.

The integrative taxonomic analysis of the *I. parvus* species complex confirmed the presence of two evolutionarily independent lineages, distinct in mtDNA sequences, nuDNA gene alleles, advertisement male call bioacoustic parameters, and ecological specialization.

These results confirm the conclusions of previous studies, which demonstrated significant differentiation within the *I. parvus* complex based on morphological data (Srion et al. 2018) and mtDNA sequences (Chan and Grismer 2019), and generally suggest the existence of two clearly defined sister species: *I. parvus* s. str. and *Ingerophrynus chrysolophus* sp. nov.

Furthermore, our study revealed that the distribution boundaries of these two species coincide with the Kangar-Pattani Line—an important biogeographic boundary separating equatorial forests from seasonal tropical monsoon forests (Morley 2000; Poyarkov et al. 2021, 2023). The Kangar-Pattani Line (KPL) is located at 6–7°N, which marks an important shift in both floristic and climatic characteristics from aseasonal to seasonal evergreen tropical forest within the Indo-Sundaic area of Southeast Asia (Van Steenis 1950; Whitmore 1984; Morley 2000; Wikramanayake et al. 2000; Woodruff 2003, 2010; Baltzer et al. 2008, 2009; Quah and Anuar 2018). It is assumed that the shift from Continental Asiatic flora in the north to Malesian flora in the south of the KPL is linked to the presence of one or more months of drought occurring north of the KPL (Whitmore 1990). The climatic forces that have shaped the flora have similarly affected the distribution of fauna in the region. Numerous studies have shown it to be a significant area for faunal exchange across various taxa, including amphibians (Quah and Anuar 2018; Poyarkov et al. 2020; Suwannapoom et al. 2020, 2021, 2022; Trofimets et al. 2024), reptiles (Grismer 2011; Grismer et al. 2014, 2020a, 2020b, 2023; Idiiatullina et al. 2023, 2024), birds (Reddy 2008), and mammals (Woodruff and Turner 2009; Patou et al. 2010). Our data further underline the importance of this biogeographic boundary in shaping the diversity of Southeast Asian amphibians.

Many new amphibian species are described every year, often by revising wide-ranging species complexes consisting of lineages with superficially similar external morphology (Trofimets et al. 2024; Gorin et al. 2024). There is no doubt that intensified survey efforts, especially in the unexplored remote mountain and island areas of Southeast Asia, coupled with the introduction of new techniques, will facilitate the discovery of overlooked diversity in the genus *Ingerophrynus* species (Evans et al. 2003). An integrative taxonomic approach appears to be crucial in analyzing the cryptic diversity of amphibians, and in the case of anurans, bioacoustic analysis is particularly promising (Koehler et al. 2017). Herein we provide brief descriptions of male advertisement calls of *I. parvus* s. str. and *Ingerophrynus chrysolophus* sp. nov. and reveal stable differences in temporal and frequency parameters among the calls of these two species. It is notable that, to date, the existing data on the bioacoustics of the genus *Ingerophrynus* are extremely scarce; to the best of our knowledge, only two papers briefly describing call parameters for *I. quadriporcatus* and *I. divergens* were published (Sukumaran et al. 2010; Amram et al. 2018). Therefore, we present the first bioacoustic data for the *I. parvus* species complex members and encourage further studies of male advertisement call variation in the genus *Ingerophrynus*.

With the description of *Ingerophrynus chrysolophus* sp. nov. and the proposed synonymization of *I. wangyingyongi* and *I. ledongensis* with *I. galeatus*, the total number of species in the genus reaches 12, three of which are known to occur in Thailand, namely *I. chrysolophus* sp. nov., *I. macrotis*, and *I. parvus* s. str. As a result of this revision, the distribution of *I. parvus* s. str. is limited to Sumatra (the entire island) and Java (the westernmost part of the island), the Malay Peninsula south of the Kangar-Pattani Line, and several offshore islands (like the Seribuat Archipelago of Malaysia). Consequently, we remove *I. parvus* from the fauna of Cambodia and Myanmar. Furthermore, two small-sized *Ingerophrynus* species, namely *I. biporcatus* and *I. divergens*, which are superficially similar to the *I. parvus* complex, have been previously reported from Peninsular Thailand without voucher specimens or detailed information on these records (Chuaynkern and Chuaynkern 2012; Poyarkov et al. 2021). We suspect that these are misidentifications of species belonging to the *I. parvus* complex, and therefore we propose to remove these two species from the fauna of Thailand pending further evidence of their occurrence.

While it is often difficult to observe consistent differences in external morphology among closely related amphibian species, studying cranial morphology shows great promise and can be particularly informative for diagnostics on different levels (e.g., Deforel et al. 2021; Gorin et al. 2021; Poyarkov et al. 2024; and the references therein). Overall, the studies on osteology of the family Bufonidae appear to be scarce, with no studies known to us dedicated to the genus *Ingerophrynus* in particular. In this regard, we hope that our current research will provide a solid framework for the subsequent revisions of the genus *Ingerophrynus* that include osteological data. Although we are lacking a reference work to provide a comparison between different species of *Ingerophrynus*, the obtained micro-CT scans provided new data on the anatomy of the supraorbital and supratympanic cranial crests—the diagnostic character of the genus *Ingerophrynus*. Also, our data show that the skull of *Ingerophrynus chrysolophus* sp. nov. shows both traces of hyperossification and underossification. It seems that both the hyperossification of the cranial roof and underossification of the otic region are more pronounced in the female specimen than in the male one. Unfortunately, without additional data, we are unaware if these differences can be attributed to sexual dimorphism or individual variability.

Most species of the genus *Ingerophrynus* have the conservation status Least Concern (LC), and only such narrow-ranged endemics as *I. kumquat* and *I. gollum* are listed as Endangered (EN) in the IUCN's Red List categories (IUCN 2019). The description of a new species of this genus emphasizes the uniqueness of the fauna of Thailand, and the occurrence of the species in different localities of the country gives reason to believe that concerns about its extinction are minimal.

Acknowledgments

We would like to thank the Laboratory Animal Research Center, University of Phayao, and the Institute of Animal for Scientific Purposes Development (IAD), Thailand, for their permission to conduct the fieldwork there. We are deeply grateful to T. Ruangsuwan, M. Naiduangchan, and T. Worranuch (Thailand), and T. Matsukoji (Japan) for their help during the field surveys. We thank the members of MSU HerpLab, including A. V. Trofimets, S. S. Idiiatullina, N. S. Kliukin, and E. N. Solovyeva, for their support and assistance. We express our sincere gratitude to the academic editor Arthur Tiutenko and Zeeshan Mirza for numerous constructive comments and suggestions, which allowed us to improve the previous version of the manuscript.

This work was supported by the Russian Science Foundation to N.A. Poyarkov (Grant No. RSF 22-14-00037-P, specimen collection and preservation, molecular and morphological analyses, and data analyses), the National Science Foundation (Grant No. NSF DEB-1146324 to E.N. Smith and M.B. Harvey), and the Thailand Science Research and Innovation Fund and the University of Phayao, Unit of Excellence 2026 on Aquatic Animals Biodiversity Assessment (Phase II) to C. Suwannapoom. Specimen collection and animal use protocols in Thailand were approved by the Institutional Ethical Committee of Animal Experimentation of the University of Phayao, Phayao, Thailand (certificate number UP-AE64-02-04-005, issued to C. Suwannapoom) and were strictly compliant with the ethical conditions of the Thailand Animal Welfare Act. Fieldwork, including the collection of animals in the field, was authorized by the Institute of Animals for Scientific Purpose Development (IAD), Bangkok, Thailand (permit numbers U1-01205-2558 and UP-AE59-01-04-0022, issued to C. Suwannapoom). Research in Indonesia was conducted under research permit 149/SIP/FRP/SM/V/2013 (issued to E.N. Smith).

References

Amram MF, Zainudin RA, Wahid HA (2018) Mating calls of selected Sarawak toads (Amphibia: Anura: Bufonidae). Sains Malaysiana 47(1): 1–7. https://doi.org/10.17576/jsm-2018-4701-01

Baltzer JL, Davies SJ, Bunyavejchewin S, Noor NSM (2008) The role of desiccation tolerance in determining tree species distributions along the Malay-Thai Peninsula. Functional Ecology 22(2): 221–231. https://doi.org/10.1111/j.1365-2435.2007.01374.x

Baltzer JL, Grégoire DM, Bunyavejchewin S, Noor NSM, Davies SJ (2009) Coordination of foliar and wood anatomical traits contributes to tropical tree distributions and productivity along the Malay-Thai Peninsula. American Journal of Botany 96(12): 2214–2223. https://doi.org/10.3732/ajb.0800414

Boulenger GA (1887) On new batrachians from Malacca. Annals and Magazine of Natural History 5: 345–348. https://doi.org/10.1080/00222938709460254

Chan KO, Grismer LL (2019) To split or not to split? Multilocus phylogeny and molecular species delimitation of southeast Asian toads (family: Bufonidae). BMC Evolutionary Biology 19(95): 1–12. https://doi.org/10.1186/s12862-019-1422-3

Chan-ard T, Cota M, Makchai S (2011) The Amphibians of the Eastern Region, With a Checklist of Thailand. National Science Museum, Pathum Thani, 160 pp. [in Thai]

Chuaynkern Y, Chuaynkern C (2012) A checklist of amphibians in Thailand. Journal of wildlife in Thailand 19(1): 163–211. [in Thai]

Das I, Lim KKP (2001) Catalogue of the herpetological types in the collection of the Raffles Museum of Biodiversity Research, National University of Singapore. Raffles Bulletin of Zoology, Singapore 49: 7–11.

Deforel F, Duport-Bru AS, Rosset SD, Baldo D, Candioti FV (2021) Osteological atlas of *Melanophryniscus* (Anura, Bufonidae): a synthesis after 150 years of skeletal studies in the genus. Herpetological Monographs 35(1): 1–27. https://doi.org/10.1655/HERPMONOGRAPHS-D-20-00002

Dufresnes C, Brelsford A, Jeffries DL, Mazepa G, Suchan T, Canestrelli D, Nicieza A, Fumagalli L, Dubey S, Martínez-Solano I, Litvinchuk SN (2021) Mass of genes rather than master genes underlie the genomic architecture of amphibian speciation. Proceedings of the National Academy of Sciences 118: e2103963118. https://doi.org/10.1073/pnas.2103963118

Dufresnes C, Poyarkov NA, Jablonski D (2023) Acknowledging more biodiversity without more species. Proceedings of the National Academy of Sciences 120: e2302424120. https://doi.org/10.1073/pnas.2302424120

Dufresnes C, Poyarkov NA, Jablonski D (2024) Reply to Lukhtanov: Polytypic species: Old wine in a new bottle. Proceedings of the National Academy of Sciences 121: e2321819121. https://doi.org/10.1073/pnas.2321819121

Elith J (2002) Quantitative methods for modeling species habitat: comparative performance and an application to Australian plants. Quantitative Methods for Conservation Biology, Springer: 39–58. https://doi.org/10.1007/0-387-22648-6_4

Evans BJ, Melnick DJ, Cannatella DC, Supriatna J, Andayani N, Setiadi MI (2003) Monkeys and toads define areas of endemism on Sulawesi. Evolution 57: 1436–1443. https://doi.org/10.1111/j.0014-3820.2003.tb00350.x

Fei L, Ye C, Jiang J (2012) Colored Atlas of Chinese Amphibians and Their Distributions. Sichuan Publishing House of Science & Technology, 596 pp. [in Chinese]

Flot JF (2010) Seqphase: a web tool for interconverting phase input/output files and fasta sequence alignments. Molecular Ecology Resources 10(1): 162–166. https://doi.org/10.1111/j.1755-0998.2009.02732.x

Frost DR (2025) Amphibian Species of the World: An Online Reference. Version 6.0. American Museum of Natural History, New York. http://research.amnh.org/herpetology/amphibia/index.html [accessed on 15 June 2025]

Frost DR, Grant T, Faivovich J, Bain RH, Haas A, Haddad CFB, de Sá RO, Channing A, Wilkinson M, Donnellan SC, Raxworthy CJ, Campbell JA, Blotto BL, Moler PE, Drewes RC, Nussbaum RA, Lynch JD, Green DM, Wheeler WC (2006) The amphibian tree of life. Bulletin of the American Museum of Natural History 297: 1–370. https://doi.org/10.1206/0003-0090(2006)297[0001:TATOL]2.0.CO;2

Goebel AM, Donnelly JM, Atz ME (1999) PCR primers and amplification methods for 12S ribosomal DNA, the control region, cytochrome oxidase I, and cytochrome b in bufonids and other frogs, and an overview of PCR primers which have amplified DNA in amphibians successfully. Molecular Phylogenetics and Evolution 11: 163–199. https://doi.org/10.1006/mpev.1998.0538

Gong SP, Wang LJ, Liao GQ, Yang CT (2011) A new Amphibian record to Guangdong Province, China—*Bufo ledongensis*. Chinese Journal of Zoology, 46: 120–123. [in Chinese]

Gorin VA, Orlov NL, Bragin AM, Pawangkhanant P, Milto KD, Le DX, Nguyen TV, Suwannapoom C, Poyarkov NA (2024) Phylogeographic pattern and taxonomic revision of the *Kaloula baleata* species complex (Amphibia: Anura: Microhylidae) with description of two new species from Indochina. Herpetozoa 37(1): 391–420. https://doi.org/10.3897/herpetozoa.37.e137394

Gorin VA, Scherz MD, Korost DV, Poyarkov NA (2021) Consequences of parallel miniaturisation in Microhylinae (Anura, Microhylidae), with the description of a new genus of diminutive South East Asian frogs. Zoosystematics and Evolution 97(1): 21–54. https://doi.org/10.3897/zse.97.57968

Grismer LL (2007) A new species of *Ingerophrynus* (Anura: Bufonidae) from a lowland rain forest in southern peninsular Malaysia. Journal of Herpetology 41: 225–230. https://doi.org/10.1670/0022-1511(2007)41[225:ANSOIA]2.0.CO;2

Grismer LL (2012) Amphibians and reptiles of the Seribuat Archipelago (Peninsular Malaysia). Frankfurt Contributions of Natural History. Vol. 50. Frankfurt am Main: Edition Chimaira, 239 pp.

Grismer LL (2011) Lizards of Peninsular Malaysia, Singapore and their Adjacent Archipelagos. Their Description, Distribution, and Natural History. Frankfurt am Main: Edition Chimaira, 728 pp.

Grismer LL, Pawangkhanant P, Idiiatullina SS, Trofimets AV, Nazarov RA, Suwannapoom C, Poyarkov NA (2023) A new species of *Cyrtodactylus* Gray, 1827 (Squamata: Gekkonidae) from the Thai-Malay Peninsula and the independent evolution of cave ecomorphology on opposite sides of the Gulf of Thailand. Zootaxa 5352(1): 109–136. https://doi.org/10.11646/zootaxa.5352.1.4

Grismer LL, Wood PL, Anuar S, Quah ES, Muin MA, Mohamed M, Chan KO, Sumarli AX, Loredo AI, Heinz HM (2014) The phylogenetic relationships of three new species of the *Cyrtodactylus pulchellus* complex (Squamata: Gekkonidae) from poorly explored regions in northeastern Peninsular Malaysia. Zootaxa 3786(3): 359–381. https://doi.org/10.11646/zootaxa.3786.3.6

Grismer LL, Yushchenko PV, Pawangkhanant P, Nazarov RA, Naiduangchan M, Suwannapoom C, Poyarkov NA (2020a) A new species of *Cnemaspis* Strauch (Squamata: Gekkonidae) of the *C. siamensis* group from Tenasserim Mountains, Thailand. Zootaxa 4852(5): 547–564. https://doi.org/10.11646/zootaxa.4852.5.3

Grismer LL, Yushchenko PV, Pawangkhanant P, Naiduangchan M, Nazarov RA, Orlova VF, Suwannapoom C, Poyarkov NA (2020b) A new species of *Hemiphyllodactylus* Bleeker (Squamata; Gekkonidae) from Peninsular Thailand that converges in morphology and color pattern on *Pseudogekko smaragdinus* (Taylor) from the Philippines. Zootaxa 4816(2): 171–190. https://doi.org/10.11646/zootaxa.4816.2.2

Günther ACLG (1864) The Reptiles of British India. London: Ray Society by R. Hardwicke, 452 pp. https://doi.org/10.5962/bhl.title.5012

Hall TA (1999) BioEdit: a user-friendly biological sequence alignment editor and analysis program for Windows 95/98/NT. Nucleic acids symposium series. Information Retrieval Ltd, London: 95–98.

Hedges SB (1994) Molecular evidence for the origin of birds. Proceedings of the National Academy of Sciences 91(7): 2621–2624. https://doi.org/10.1073/pnas.91.7.2621

Hillis DM, Moritz C, Mable BK (1996) Molecular Systematics, 2nd edn. Sinauer, Sunderland, Massachsetts, 655 pp. https://doi.org/10.2307/1447682

Holden J (2023) Amphibians of Cambodia. A Field Guide. Frankfurt Contributions of Natural History. Vol. 91. Frankfurt am Main: Edition Chimaira, 256 pp.

Huelsenbeck JP, Hillis DM (1993) Success of phylogenetic methods in the four-taxon case. Systematic Biology 42(3): 247–264. https://doi.org/10.1093/sysbio/42.3.247

Huelsenbeck JP, Ronquist F (2001) MRBAYES: Bayesian inference of phylogenetic trees. Bioinformatics 17(8): 754–755. https://doi.org/10.1093/bioinformatics/17.8.754

Idiiatullina SS, Pawangkhanant P, Tawan T, Worranuch T, Dechochai B, Suwannapoom C, Nguyen TV, Chanhome L, Poyarkov NA (2023) Limestone jewel: A new colourful karst-dwelling pitviper (Serpentes: Viperidae: *Trimeresurus*) from the poorly explored borderlands of southern peninsular Thailand. Vertebrate Zoology 73: 697–716. https://doi.org/10.3897/vz.73.e109854

Idiiatullina SS, Nguyen TV, Pawangkhanant P, Suwannapoom C, Chanhome L, Mirza ZA, David P, Vogel G, Poyarkov NA (2024) An integrative taxonomic revision of the *Trimeresurus popeiorum* group of pitvipers (Reptilia: Serpentes: Viperidae) with descriptions of two new species from the Indo-Burma Biodiversity Hotspot. Vertebrate Zoology 74: 303–342. https://doi.org/10.3897/vz.74.e113347

Inger RF (1966) The systematics and zoogeography of the Amphibia of Borneo. Fieldiana Zoology 52: 1–402. https://doi.org/10.5962/bhl.title.3147

Inger RF (1972) *Bufo* of Eurasia. In: Blair WF (Ed.) Evolution in the Genus *Bufo*. Austin and London, University of Texas Press, 102–118.

Iskandar DT (1998) The Amphibians of Java and Bali. Research and Development Centre for Biology-LIPI, 46 pp.

IUCN Standards and Petitions Committee (2019) Guidelines for Using the IUCN Red List Categories and Criteria. Version 14. Prepared by the Standards and Petitions Committee, 122 pp.

Kalyaanamoorthy S, Minh BQ, Wong TK, Von Haeseler A, Jermiin LS (2017) ModelFinder: fast model selection for accurate phylogenetic estimates. Nature methods 14(6): 587–589. https://doi.org/10.1038/nmeth.4285

Koehler J, Jansen M, Rodriguez A, Kok PJ, Toledo LF, Emmrich M, Glaw F, Haddad CF, Roedel MO, Vences M (2017) The use of bioacoustics in anuran taxonomy: theory, terminology, methods, recommendations for best practice. Zootaxa 4251(1): 1–124. https://doi.org/10.11646/zootaxa.4251.1.1

Leigh JW, Bryant D (2015) POPART: Full-feature software for haplotype network construction. Methods in Ecology and Evolution 6: 1110–1116. https://doi.org/10.1111/2041-210X.12410

Liedtke HC, Müller H, Hafner J, Penner J, Gower DJ, Mazuch T, Rödel MO, Loader SP (2017) Terrestrial reproduction as an adaptation to steep terrain in African toads. Proceedings of the Royal Society B: Biological Sciences 284(1851): 20162598. https://doi.org/10.1098/rspb.2016.2598

Liu S, Zhang L, Ananjeva NB, Liu Z, Hou M, Orlov NL (2025) A new species of *Ingerophrynus* (Anura, Bufonidae) from Guangdong, China. Russian Journal of Herpetology 32: 85–95. https://doi.org/10.30906/1026-2296-2025-32-2-85-95

Manthey U, Grossmann W (1997) Amphibien und Reptilien Südostasiens. Münster, Natur und Tier–Verlag, 512 pp. [in German]

Meewattana P (2022) Anuran Tadpoles of Thailand: Field Guide and Key. We Plus Group, Samut Prakan, 238 pp.

Minh BQ, Nguyen MAT, Von Haesele A (2013) Ultrafast approximation for phylogenetic bootstrap. Molecular biology and evolution 30(5): 1188–1195. https://doi.org/10.1093/molbev/mst024

Morley RJ (2000) Origin and evolution of tropical rain forests. Chichester, United Kingdom: John Wiley & Sons, 362 pp.

Mouhot MH (1864) Travels in the Central Parts of Indo-China (Siam), Cambodia, and Laos, during the Years 1858, 1859, and 1860. John Murray, London, Vol. I, 303 pp., Vol. II, 301 pp.

Mulcahy DG, Lee JL, Miller AH, Chand M, Thura MK, Zug GR (2018) Filling the BINs of life: report of an amphibian and reptile survey of the Tanintharyi (Tenasserim) Region of Myanmar, with DNA barcode data. ZooKeys (757): 85–152. https://doi.org/10.3897/zookeys.757.24453

Neang T, Holden J (2008) A Field Guide to the Amphibians of Cambodia. Fauna & Flora International, Phnom Penh, 127 pp.

Nguyen LT, Schmidt HA, Von Haeseler A, Minh BQ (2015) IQ-TREE: a fast and effective stochastic algorithm for estimating maximum-likelihood phylogenies. Molecular biology and evolution 32(1): 268–274. https://doi.org/10.1093/molbev/msu300

Nishikawa K, Matsui M, Tanabe S, Sato SI (2007) Morphological and allozymic variation in *Hynobius boulengeri* and *H. stejnegeri* (Amphibia: Urodela: Hynobiidae). Zoological Science 24(7): 752–766. https://doi.org/10.2108/zsj.24.752

Niyomwan P, Srisom P, Pawangkhanant P (2019) Field Guide to the Amphibians of Thailand. Parb Phim Printing, Bangkok, 485 pp. [in Thai]

Ohler A, Swan SR, Daltry JC (2002) A recent survey of the amphibian fauna of the Cardamom Mountains, Southwest Cambodia with descriptions of three new species. Raffles Bulletin of Zoology, Singapore 50: 465–481.

Páez-Moscoso DJ, Guayasamin JM (2012) Species limits in the Andean toad genus *Osornophryne* (Bufonidae). Molecular Phylogenetics and Evolution 65(3): 805–822. https://doi.org/10.1016/j.ympev.2012.08.001

Patou ML, Wilting A, Gaubert P, Esselstyn JA, Cruaud C, Jennings AP, Fickel J, Veron G (2010) Evolutionary history of the *Paradoxurus* palm civets–a new model for Asian b https://doi.org/10.1111/j.1365-2699.2010.02364.x iogeography. Journal of Biogeography 37(11): 2077–2097.

Phillips SJ, Anderson RP, Schapire RE (2006) Maximum entropy modeling of species geographic distributions. Ecological modelling 190(3–4): 231–259. https://doi.org/10.1016/j.ecolmodel.2005.03.026

Phillips SJ, Dudík M (2008) Modeling of species distributions with Maxent: new extensions and a comprehensive evaluation. Ecography 31(2): 161–175. https://doi.org/10.1111/j.0906-7590.2008.5203.x

Poyarkov NA, Nguyen TV, Le SX, Le D, Arkhipov D, Gorin VA, Hernandez A, Dufresnes C (2024) Multiple lines of evidence for a new cryptic species of *Tylototriton* (Amphibia, Salamandridae) from northern Vietnam. Alytes 41(1–4): 56–98. https://doi.org/10.47605/tapro.v10i1.244

Poyarkov NA, Nguyen TV, Popov ES, Geissler P, Pawangkhanant P, Neang T, Suwannapoom C, Orlov NL (2021) Recent progress in taxonomic studies, biogeographic analysis and revised checklist of amphibians in Indochina. Russian Journal of Herpetology 28(3A): 1–110. https://doi.org/10.30906/1026-2296-2021-28-3A-1-110

Poyarkov NA, Nguyen TV, Popov ES, Geissler P, Pawangkhanant P, Neang T, Suwannapoom C, Ananjeva NB, Orlov NL (2023) Recent progress in taxonomic studies, biogeographic analysis and revised checklist of reptiles in Indochina. Russian Journal of Herpetology 30(5): 255–476. https://doi.org/10.30906/1026-2296-2023-30-5-255-476

Poyarkov NA, Pawangkhanant P, Gorin VA, Juthong W, Suwannapoom C (2020) A new species of miniaturised narrow-mouth frog of the genus *Microhyla* Tschudi, 1838 (Amphibia: Anura: Microhylidae) from northern Tenasserim, Thailand. Journal of Natural History 54(23–24): 1525–1558. https://doi.org/10.1080/00222933.2020.1804005

Pramuk JB (2006) Phylogeny of South American *Bufo* (Anura: Bufonidae) inferred from combined evidence. Zoological journal of the Linnean Society 146(3): 407–452. https://doi.org/10.1111/j.1096-3642.2006.00212.x

Pregill G (1981) Cranial morphology and the evolution of West Indian toads (Salientia: Bufonidae): resurrection of the genus *Peltophryne* Fitzinger. Copeia 1981(2): 273–285. https://doi.org/10.2307/1444216

QGIS Development Team (2021) QGIS geographic information system. Open Source Geospatial Foundation Project. http://qgis.osgeo.org [accessed on 15 June 2025]

Quah ES, Anuar MS (2018) Herpetofauna of the northern corridor: a review of recent herpetological discoveries around the Malaysian-Thai border regions. Journal of Wildlife and Parks 33: 15–29.

Raven Pro: Interactive Sound Analysis Software (Version 1.6.5) [Computer software]. Ithaca, NY: The Cornell Lab of Ornithology. https://www.ravensoundsoftware.com/

Reddy S (2008) Systematics and biogeography of the shrike-babblers (*Pteruthius*): species limits, molecular phylogenetics, and diversification patterns across southern Asia. Molecular Phylogenetics and Evolution 47(1): 54–72. https://doi.org/10.1016/j.ympev.2008.01.014

Ronquist F, Huelsenbeck JP (2003) MrBayes 3: Bayesian phylogenetic inference under mixed models. Bioinformatics 19(12): 1572–1574. https://doi.org/10.1093/bioinformatics/btg180

Sambrook J, Russel DW (2001) Molecular Cloning: A Laboratory Manual. CSHL Press, New York, 1890 pp.

Sarker GC, Wostl E, Thammachoti P, Sidik I, Hamidy A, Kurniawan N, Smith EN (2019) New species, diversity, systematics, and conservation assessment of the Puppet Toads of Sumatra (Anura: Bufonidae: *Sigalegalephrynus*). Zootaxa 4679(2): 365–391. https://doi.org/10.11646/zootaxa.4679.2.9

Savage JM (1975) Systematics and distribution of the Mexican and Central American stream frogs related to *Eleutherodactylus rugulosus*. Copeia 1975: 254–306. https://doi.org/10.2307/1442883

Smart U, Sarker GC, Arifin U, Harvey MB, Sidik I, Hamidy A, Kurniawan N, Smith EN (2017) A new genus and two new species of arboreal toads from the highlands of Sumatra with a phylogeny of Sundaland toad genera. Herpetologica 73(1): 63–75. https://doi.org/10.1655/Herpetologica-D-16-00041

Srion L, Wangkulangkul S, Aowphol A (2018) Morphological Variation of *Ingerophrynus parvus* (Boulenger, 1887) in peninsular Thailand. IOP Conference Series: Earth and Environmental Science 197 (012011): 1–7. https://doi.org/10.1088/1755-1315/197/1/012011

Stephens M, Smith NJ, Donnelly P (2001) A new statistical method for haplotype reconstruction from population data. American Journal of Human Genetics 68(4): 978–989. https://doi.org/10.1086/319501

Stuart BL, Sok K, Neang T (2006) A collection of amphibians and reptiles from hilly eastern Cambodia. Raffles Bulletin of Zoology. Singapore 54: 129–155.

Sukumaran J, Das I, Haas A (2010) Descriptions of the advertisement calls of some Bornean frogs. Russian Journal of Herpetology 17(3): 189–194.

Suwannapoom C, Grismer LL, Pawangkhanant P, Naiduangchan M, Yushchenko PV, Arkhipov DV, Poyarkov NA (2021) Hidden tribe: A new species of Stream Toad of the genus *Ansonia* Stoliczka, 1870 (Anura: Bufonidae) from the poorly explored mountainous borderlands of western Thailand. Vertebrate Zoology 71: 763–779. https://doi.org/10.3897/vz.71.e73529

Suwannapoom C, Grismer LL, Pawangkhanant P, Poyarkov NA (2022) A new species of stream toad of the genus *Ansonia* Stoliczka, 1870 (Anura: Bufonidae) from Nakhon Si Thammarat Range in southern Thailand. Zootaxa 5168(2): 119–136. https://doi.org/10.11646/zootaxa.5168.2.2

Suwannapoom C, Nguyen VT, Pawangkhanant P, Gorin VA, Chomdej S, Che J, Poyarkov NA (2020) A new species of *Micryletta* (Amphibia: Microhylidae) from southern Thailand. Zoological Research 41(5): 581–588. https://doi.org/10.24272/j.issn.2095-8137.2020.139

Swets JA (1988) Measuring the accuracy of diagnostic systems. Science 240(4857): 1285–1293. https://doi.org/10.1126/science.3287615

Tamura K, Stecher G, Peterson D, Filipski A, Kumar S (2013) MEGA6: molecular evolutionary genetics analysis version 6.0. Molecular biology and evolution 30(12): 2725–2729. https://doi.org/10.1093/molbev/mst197

Taylor EH (1962) The amphibian fauna of Thailand. University of Kansas Science Bulletin 43: 324–326. https://doi.org/10.5962/bhl.part.13347

Thompson JD, Higgins DG, Gibson TJ (1994) CLUSTAL W: improving the sensitivity of progressive multiple sequence alignment through sequence weighting, position-specific gap penalties and weight matrix choice. Nucleic acids research 22(22): 4673–4680. https://doi.org/10.1093/nar/22.22.4673

Trofimets AV, Dufresnes C, Pawangkhanant P, Bragin AM, Gorin VA, Hasan M, Lalremsanga HT, Muin MA, Le DX, Nguyen TV, Suwannapoom C, Poyarkov NA (2024) Four in one: an integrative taxonomic revision of the *Microhyla berdmorei* complex (Amphibia: Anura: Microhylidae) illustrates the tremendous amphibian diversity of Southeast Asia. Vertebrate Zoology 74: 595–641. https://doi.org/10.3897/vz.74.e127937

Trueb L (1973) Bones, frogs, and evolution. In: Evolutionary biology of the anurans: contemporary research on major problems. University of Missouri Press, 65–132.

Van der Meijden A, Vences M, Hoegg S, Boistel R, Channing A, Meyer A (2007) Nuclear gene phylogeny of narrow-mouthed toads (Family: Microhylidae) and a discussion of competing hypotheses concerning their biogeographical origins. Molecular Phylogenetics and Evolution 44: 1017–1030. https://doi.org/10.1016/j.ympev.2007.02.008

Van Steenis CGGJ (1950) The delimitation of Malaysia and its main plant geographical divisions. In: Van Steenis CGGJ (Ed.) Flora Malesiana, Series 1 (Spermatophyta), 1: 70–75. https://doi.org/10.5962/bhl.title.40744

Vences M, Thomas M, Bonett RM, Vieites DR (2005) Deciphering amphibian diversity through DNA barcoding: chances and challenges. Philosophical Transactions of the Royal Society 360(1462): 1859–1868. https://doi.org/10.1098/rstb.2005.1717

Vieites DR, Wollenberg KC, Andreone F, Köhler J, Glaw F, Vences M (2009) Vast underestimation of Madagascar's biodiversity evidenced by an integrative amphibian inventory. Proceedings of the National Academy of Sciences 106(20): 8267–8272. https://doi.org/10.1073/pnas.0810821106

Warren DL, Glor RE, Turelli M (2010) ENMTools: a toolbox for comparative studies of environmental niche models. Ecography 33: 607–611. https://doi.org/10.1111/j.1600-0587.2009.06142.x

Whitmore TC (1984) Tropical Rainforests of the Far East, 2nd edn. Oxford, United Kingdom: Oxford University Press, 366 pp.

Whitmore TC (1990). An introduction to tropical rain forests. Oxford, United Kingdom: Clarendon Press, 226 pp.

Wiens JJ, Reeder TW, Fetzner JW, Parkinson CL, Duellman WE (2005) Hylid frog phylogeny and sampling strategies for speciose clades. Systematic Biology 54: 719–748. https://doi.org/10.1080/10635150500234625

Wikramanayake E, Dinerstein E, Loucks C, Olson D, Morrison J, Lamoreux J, McKnight M, Hedao P (2000) Terrestrial Ecoregions of the Indo-Pacific: A Conservation Assessment. Island Press, Washington, DC, 643 pp.

Woodruff DS, Turner LM (2009) The Indochinese–Sundaic zoogeographic transition: a description of terrestrial mammal species distributions. Journal of Biogeography 36: 803–821. https://doi.org/10.1111/j.1365-2699.2008.02071.x

Woodruff DS (2003) The location of the Indochinese-Sundaic biogeographic transition in plants and birds. Natural History Bulletin of Siam Society 51(1): 97–108.

Woodruff DS (2010) Biogeography and conservation in Southeast Asia: how 2.7 million years of repeated environmental fluctuations affect today's patterns and the future of the remaining refugial-phase biodiversity. Biodiversity Conservation 19: 919–941. https://doi.org/10.1007/s10531-010-9783-3

Zug GR (2022) Amphibians and reptiles of Myanmar: Checklists and keys I. Amphibians, crocodilians and turtles. Smithsonian Contributions to Zoology 653: 1–113. https://doi.org/10.5479/si.19098995

Zug GR, Mulcahy DG (2020) The Amphibians and Reptiles of South Tanintharyi. Cambridge: Fauna & Flora International, 203 pp.

Supplementary material 1

Supplementary information

Authors: Dmitriy V. Arkhipov, Parinya Pawangkhanant, Goutam Sarker, Vladislav A. Gorin, Andrey M. Bragin, Tan Van Nguyen, Amir Hamidy, Mohd Abdul Muin, Nia Kurniawan, Rafe M. Brown, Chatmongkon Suwannapoom, Eric Smith, Nikolay A. Poyarkov

Data type: docx

Copyright notice: This dataset is made available under the Open Database License (http://opendatacommons.org/licenses/odbl/1.0/). The Open Database License (ODbL) is a license agreement intended to allow users to freely share, modify, and use this Dataset while maintaining this same freedom for others, provided that the original source and author(s) are credited.

Link: https://doi.org/10.3897/herpetozoa.38.e165173.suppl1